Photochemistry and Photobiology, 2023, 99: 235–250

Special Issue Invited Review

An Update on General Chemiexcitation Mechanisms in Cyclic Organic Peroxide Decomposition and the Chemiluminescent Peroxyoxalate Reaction in Aqueous Media†

Maidileyvis C. Cabello[1], Fernando H. Bartoloni[2] and Wilhelm J. Baader[1]*

[1]Departamento de Química Fundamental, Instituto de Química, Universidade de São Paulo, São Paulo, Brazil
[2]Centro de Ciências Naturais e Humanas, Universidade Federal do ABC, Santo André, Brazil

Received 28 May 2022, accepted 12 July 2022, DOI: 10.1111/php.13673

ABSTRACT

Four-membered ring peroxides are intimately linked to chemiluminescence and bioluminescence transformations, as high-energy intermediates responsible for electronically excited-state formation. The synthesis of 1,2-dioxetanes and 1,2-dioxetanones enabled mechanistic studies on their decomposition occurring with the formation of electronically excited carbonyl products in the singlet or triplet state. The third member of this family, 1,2-dioxetanedione, has been postulated as the intermediate in the peroxyoxalate reaction, recently confirmed by kinetic studies on peroxalic acid derivatives. Several general chemiexcitation mechanisms have been proposed as model systems for the chemiexcitation step in efficient bioluminescence and chemiluminescence transformations. In this review article, we discuss the validity and efficiency of the most important chemiexcitation mechanisms, extended to aqueous media, where the efficiency is known to be drastically reduced, specifically in the peroxyoxalate reaction, highly efficient in anhydrous environment, but much less efficient in aqueous media. Mechanistic studies of this reaction will be discussed in diverse aqueous environments, with special attention to the catalysis involved in the thermal reaction leading to the formation of the high-energy intermediate and to the chemiexcitation mechanism, as well as emission quantum yields. Finally, several recent analytical and bioanalytical applications of the peroxyoxalate reaction in aqueous media will be given.

INTRODUCTION

This review aimed to give the reader a general impression of the state-of-the-art in chemiexcitation, outlining, after a brief historical introduction, the main chemiexcitation mechanism in cyclic organic peroxide decomposition. The reader will understand that the unimolecular peroxide decomposition is not a model for efficient chemiluminescence (CL) and bioluminescence (BL), as this process leads to the preferential formation of weakly emissive triplet-excited carbonyl compounds. Whereas electron transfer catalyzed peroxide decomposition leads to preferential singlet-excited state formation with possible high emission efficiency, although it appears that this process is generally of low efficiency when it occurs in an intermolecular fashion. Contrarily, when the electron transfer process in peroxide decomposition occurs in an intramolecular manner, as in the induced decomposition of phenoxy-substituted 1,2-dioxetanes, chemiexcitation yield can be as high as 100%. A notable exception to this *status quo*, in which intramolecular processes are efficient whereas intermolecular ones are inefficient, is the peroxyoxalate CL (PO-CL) system. Chemiexcitation in PO-CL involves intermolecular electron or charge-transfer steps; however, it is highly efficient in generating light, with emission quantum yields of up to 100%. The emission quantum yields of the PO-CL reaction are much lower, however, in aqueous environments, which are present in many analytical and all bioanalytical applications of CL, and the PO-CL transformation comprises a significant part of such applications. Therefore, here we briefly introduce the main chemiexcitation mechanisms in peroxide decomposition and its efficiency, with specific attention to the PO-CL system. Then, we discuss the most recent kinetic studies of the peroxyoxalate reaction in aqueous environments, followed by recent examples of analytical and bioanalytical applications of this CL transformation.

GENERAL CHEMIEXCITATION MECHANISMS

Short history of CL

"Bioluminescence (BL) and chemiluminescence (CL) are truly spectacular phenomena and well-known to most people, although maybe not by the name. A chemical reaction producing a light-emitting product is called chemiluminescent." "Similarly, bioluminescence is the production and emission of light in living organisms" (1). Bioluminescence can be found in many animals like firefly beetles or worms, but mainly in the sea in jellyfishes, crustaceans, or mollusks but also in fungi and bacteria (2). Long-known CL transformations include lophine autoxidation (3), transition-metal catalyzed luminol oxidation (4), reaction of lucigenin with hydrogen peroxide (5) and the highly efficient peroxyoxalate reaction (6,7). All these CL reactions are widely

*Corresponding author email: wjbaader@iq.usp.br (Wilhelm J. Baader)
†This article is part of a Special Issue celebrating the 50th Anniversary of the American Society for Photobiology.

utilized in diverse analytical applications. They consist in complex parallel and consecutive reaction steps, which lead to forming an intermediate with high-energy content, responsible for the formations of electronically excited states. These high-energy intermediates (HEI) are always cyclic peroxide species, at least in the case of efficient CL transformations (8).

However, the identity of the HEI in specific reactions is unknown in many cases of CL and still more BL transformations due to the complex nature of the transformation and the low stability of these intermediates. Still, less has been known about the mechanism of excited-state formations until the synthesis of some analogs of the cyclic peroxides postulated as the HEI in CL transformations in the second part of the last century.

The preparation of four-membered cyclic peroxides as models for HEI in BL and CL transformations can be considered as an initial milestone in mechanistic CL research, with the first synthesis of a 1,2-dioxetane (**1**) derivative, trimethyl-1,2-dioxetane, by Kopecky and Mumford (9), and a 1,2-dioxetanone (**2**) (Fig. 1) derivative, the *tert*-butyl-1,2-dioxetanone, by Adam and Liu (10). Thereafter, mainly during the 70's and 80's of the last century, more than a hundred 1,2-dioxetane derivatives (11,12), including the unsubstituted, parent derivative 1,2-dioxetane (13), have been synthesized and their stability and CL properties studied. Contrarily, only some derivatives of the much less stable 1,2-dioxetanone structure have been synthesized and studied, some relatively recently (14). The third member of the four-membered cyclic peroxide family, 1,2-dioxetanedione (**3**) (Fig. 1), has been early postulated as the high-energy intermediate in the peroxyoxalate reaction (7), and evidence for its real existence accumulated during subsequent years (15–20), including quite recent direct evidence from Hammett studies on peracid derivatives (21).

Studies on the thermal and CL properties of these cyclic peroxides, isolated or formed *in situ*, contributed decisively to formulating the main general chemiexcitation mechanisms nowadays utilized to rationalize excited-state formation in bioluminescent and chemiluminescent transformations.

Mechanisms of excited-state formation

Unimolecular decomposition of cyclic peroxides. Studies on thermal stability and chemiexcitation quantum yields of hundreds of 1,2-dioxetane and half a dozen of 1,2-dioxetanone derivatives revealed the occurrence of chemiexcitation in the unimolecular decomposition with the preferential formation of triplet-excited carbonyl compounds (Scheme 1) (12,22). The mechanism of this decomposition can be considered as a concerted [2 + 2] retrocycloaddition, which would easily account for the observed excited-state formation according to the Woodward-Hoffmann rules (23), although 1,2-dioxetane stability data have indicated the possible occurrence of a stepwise biradical mechanism (24,25), whereas a concerted biradical-like mechanism appears to account for all available experimental data (26). Several theoretical studies have shown the importance of the entropic trap for chemiexcitation (1). However, unimolecular cyclic peroxide

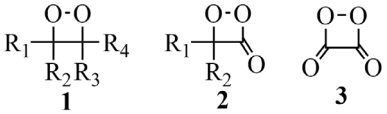

Figure 1. Four-membered cyclic peroxide structures.

decomposition cannot be used as a simple chemical model for BL transformations and complex CL reactions, as this process leads to of very low amounts of singlet-excited carbonyl products and preferential triplet-excited product formation, which are weakly emissive in aerated solution. Therefore, unimolecular cyclic peroxide decomposition is not an adequate model system for efficient BL and CL transformations.

Catalyzed peroxide decomposition: The intermolecular CIEEL mechanism. During the studies on the CL properties of four-membered cyclic peroxides, it was observed that 1,2-dioxetanones and other linear and cyclic peroxides can be subject to catalyzed decomposition in the presence of appropriate fluorescent compounds with low oxidation potentials (27,28). This catalyzed peroxide decomposition was shown to lead to the preferential formation of the singlet-excited state of fluorescent compound, called activator (ACT) (28,29). These experimental observations led to the formulation of a new chemiexcitation mechanism in the catalyzed peroxide decomposition, the Chemically Initiated Electron Exchange Luminescence (CIEEL), where peroxide decomposition is initiated, after charge-transfer complex formation, by an electron transfer from the ACT to the peroxidic O–O σ* bond, leading to O–O bond cleavage and formation of a radical-ion pair, within the solvent cage. Cleavage of the former peroxide ring C-C bond, with the liberation of a neutral species, leaves a new radical-ion pair still within the solvent cage. An electron back-transfer from the carbonyl radical anion to the ACT radical cation leads to the formation of the ACT's electronically excited singlet state (ACT^{S1}), whose fluorescence is responsible for the observed CL emission (Scheme 2) (28).

This elegant mechanistic proposal has been utilized since its formulation to rationalize excited-state formation in a vast number of CL systems and has also been applied for many BL transformations, most prominently in the firefly BL (30). Alternatively, the occurrence of charge-transfer, instead of "full" electron-transfer steps has been suggested (31–33).

However, more recently it has been observed that the quantum yields, initially measured for the catalyzed decomposition of 1,2-dioxetanones, had been overestimated in several orders of magnitude, thereby questioning the efficiency of this mechanistic proposal and its validity as model for efficient BL and CL transformations (34). Nonetheless, the occurrence of electron or charge-transfer processes in the catalyzed decomposition has been confirmed and steric repulsion for charge-transfer complex stability has been suggested as a reason for the low quantum efficiency (35,36). It has also been shown that the low quantum yields obtained in these processes are not mainly due to solvent-cage escape of radical pair during the electron/charge-transfer and back-transfer processes, as solvent viscosity effects on the singlet quantum yields in these intermolecular CIEEL system are relatively low (37–39).

Contrarily to the low-efficient intermolecular CIEEL systems outlined above, the peroxyoxalate reaction (base-catalyzed reaction of aromatic oxalate esters with hydrogen peroxide in the presence of an ACT) constitutes a highly efficient chemiexcitation system, which occurs by an intermolecular electron transfer and back-transfer sequence. The high quantum yields of up to 0.5 E mol^{-1} have been confirmed by various research groups (7,40–43), and the involvement of an electron or charge transfer been shown unequivocally (41,44,45).

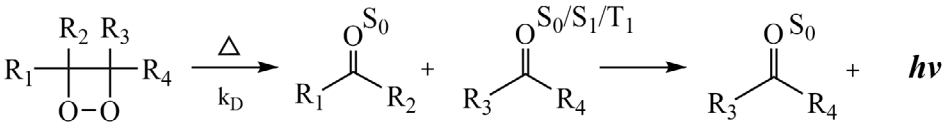

R_1, R_2 = alkyl, aryl or =O
R_3, R_4 = alkyl, aryl

Scheme 1. Unimolecular decomposition of 1,2-dioxetanes and 1,2-dioxetanones.

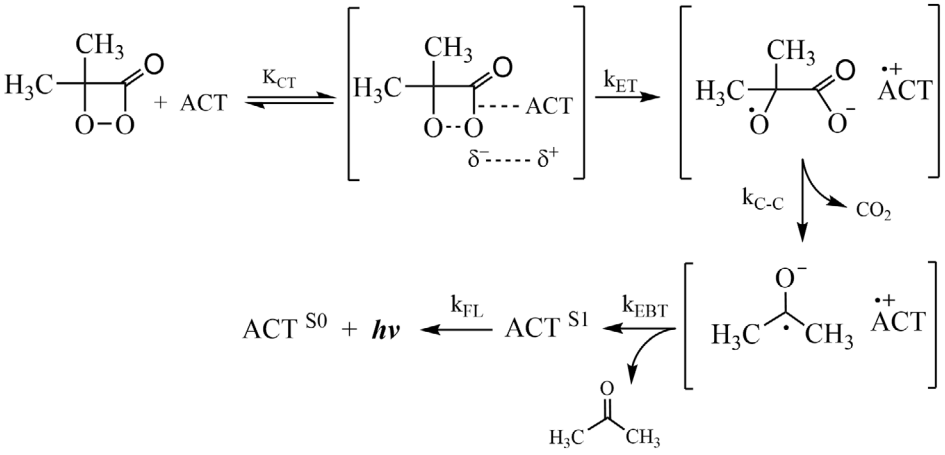

Scheme 2. Chemically initiated electron exchange luminescence (CIEEL) for the catalyzed decomposition of dimethyl-1,2-dioxetanone in the presence of a fluorescent activator (ACT). CT, charge transfer; ET, electron transfer; EBT, electron back-transfer; and Fl, fluorescence.

Induced decomposition of phenoxy-substituted 1,2-dioxetane derivatives: The intramolecular CIEEL mechanism. 1,2-Dioxetanes (**1**), contrarily to 1,2-dioxetanones (**2**), do not undergo catalyzed decomposition in the presence of easily oxidizable ATCs (22); however, when the electron donor moiety is covalently linked to the peroxidic ring, peroxide decomposition can occur, leading to the efficient formation of singlet-excited cleavage products and intense CL emission (46). The molecular design of 1,2-dioxetanes containing phenolic substituents with protective groups, which can be removed with chemical or enzymatic deprotection (47–49), leads to very efficient singlet chemiexcitation, with quantum yields, which can reach the maximum value of 1.0 E mol^{-1} (50–52). This kind of 1,2-dioxetanes has been widely utilized in bioanalytical applications, most prominently in immunoassays using phosphatase sensitive protective groups and in bioimaging (53–56). It has been shown that the reaction sequence is initiated by an intramolecular electron or charge transfer from the electron rich substituent (typically a phenolate ion) to the cyclic peroxide (57). The electron back-transfer step should also occur in an intramolecular fashion (37,58), although initial results on the solvent-cage effect in induced 1,2-dioxetane decomposition appeared to indicate an intermolecular process (Scheme 3) (59,60).

Peroxyoxalate reaction

The peroxyoxalate system, base-catalyzed reaction of aromatic oxalate esters with hydrogen peroxide in the presence of a fluorescent activator is one of the most efficient CL transformations known and the only one which occurs by the intermolecular CIEEL mechanism with certified high chemiexcitation efficiency in anhydrous medium (7,40,41,50). The chemical reaction mechanism has been well studied under different experimental conditions (61–67), leading to the formation of a high-energy intermediate (HEI). The interaction of this intermediate with the ACT generates enough energy to promote the latter to its electronically excited singlet state, which is responsible for the emission of the peroxyoxalate CL (PO-CL). (Scheme 4) (15).

The structure of the high-energy intermediate has been in discussion during the years (15); after the initial suggestion of the Rauhut group of 1,2-dioxetanedione (7), several other structural proposals for the HEI have been made, including diverse cyclic peroxides and peracid derivatives (15–19,22,68,69). However, as already mentioned above, recent Hammett studies have given direct evidence on 1,2-dioxetanedione (**3**) as the structure of the high-energy intermediate in the peroxyoxalate system (21). It has also been shown that the chemiexcitation mechanism of the peroxyoxalate reaction involves a rate-limiting electron or charge transfer, where the electronically excited state of the ACT is formed by its interaction with the HEI (41,42,44,45). Therefore, the highly efficient peroxyoxalate reaction, with proven high quantum yields in anhydrous medium, as determined by various research groups during the years (7,40–43), constituted the only efficient CL system, which occurs according to the intermolecular CIEEL mechanism.

The kinetics of the reaction in anhydrous media have been extensively studied and characterized, using different oxalate esters, nucleophilic and non-nucleophilic bases and activators (ACT, mainly polycyclic aromatic hydrocarbons), and these studies have been reviewed (15). The measured observed rate constants (k_{obs}), determined from the emission intensity *versus* time kinetic curves (Fig. 2), correspond to the relatively slow reaction

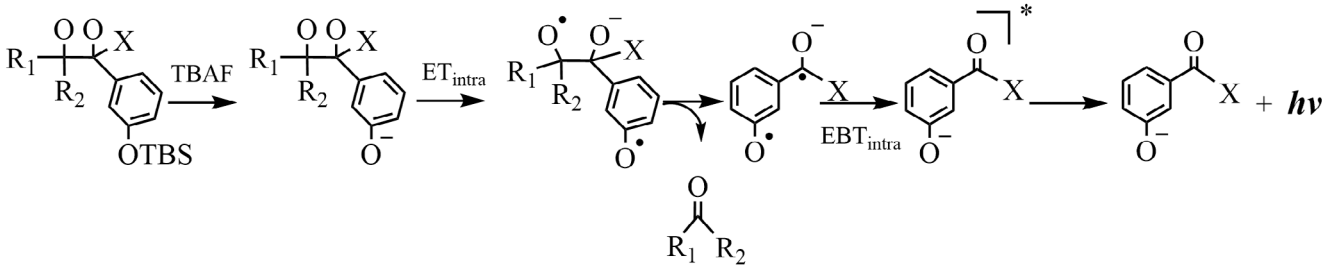

Scheme 3. Induced decomposition of phenoxy-substituted 1,2-dioxetanes occurring by an entirely intramolecular reaction pathway. X, OCH_3; H, alkyl; TBS, *tert.*-butyldimethylsilyl; TBAF, tetrabutylammonium fluoride; ET_{intra}, intramolecular electron transfer; EBT_{intra}, intramolecular electron back-transfer.

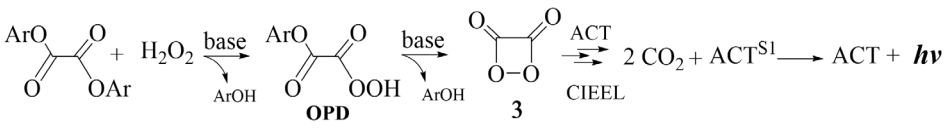

Ar = phenyl with electron-withdrawing substituents

Scheme 4. Typical peroxyoxalate system in anhydrous medium where base-catalyzed reaction of an aromatic oxalic ester, containing good phenolic leaving groups, with hydrogen peroxide results in the formation of an oxalic peracid derivative (OPD), whose base-catalyzed cyclization leads to formation of 1,2-dioxetanedione **(3)** as the high-energy intermediate. Interaction of **3** with the activator (ACT), involving the CIEEL sequence gives rise to the ACT's electronically excited singlet state (ACT_{S1} whose fluorescence is responsible for the CL emission.

steps, which lead to the formation of the high-energy intermediate. Depending on the reaction conditions, two k_{obs} values can be extracted from the kinetic curves, one for the rise in CL intensity and the other for the fall, and these can be attributed to specific steps in the kinetic Scheme (15). Furthermore, as k_{obs} values may change with respect to a planned systematic variation in reagents' concentrations, bi and trimolecular rate constants associated to specific reaction steps can be determined (15). The chemiluminescence emission quantum yields (Φ_{CL}, quantum of light emitted per mol of limiting reagent, commonly, the oxalate ester) are determined from the integral of the CL emission intensity curve, using the luminol standard for calibration of the detection device (15,41,50). The singlet quantum yields (Φ_S, quantum yield of singlet-excited state formation per mol of limiting reagent) are obtained from the Φ_{CL} by considering the fluorescence emission quantum yield of the ACT (Φ_{Fl}), where $\Phi_S = \Phi_{CL}/\Phi_{Fl}$. The kinetics of the chemiexcitation step cannot be measured in the complete peroxyoxalate system, as this step is much faster than the preceding ones; however, using a special arrangement, it was possible to obtain rate constants for this step, which showed to depend on the activator concentration and its oxidation potential, indicating that it involves an electron or charge transfer (44). The efficiency of the chemiexcitation step appears to depend on the energy liberated in this step by the electron back-transfer from the carbonyl radical anion to the ACT's radical cation (Scheme 2) (41,42).

On the other hand, if the peroxyoxalate reaction is performed in aqueous media, which would be important for analytical and bioanalytical applications, the quantum yields have been shown to be several orders of magnitude lower and the reactions considerably faster compared to anhydrous conditions (15); compare, for instance, the kinetic emission curves for the same PO-CL reaction in organic solvent and aqueous mixture (Fig. 2). Moreover, it has been shown recently that the low quantum yields in aqueous medium are not predominantly due to the occurrence of oxalate ester hydrolysis, but are, apparently, due to the low

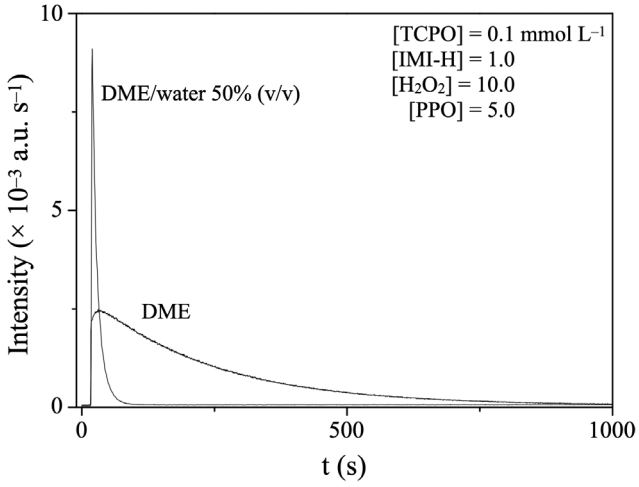

Figure 2. Emission intensity *versus* time curves for the same PO-CL system, with respect to reagents and their concentrations, in anhydrous 1,2-dimethoxyethane (DME) and in DME/water 50% (v/v). The volumetric ratio of DME/water 50% (v/v) corresponds to a mixture containing 85% of water in moles, *that is*, DME/water 15/85 (n/n). Reagents are bis (2,4,6-trichlorophenyl) oxalate (TCPO), imidazole (IMI-H), hydrogen peroxide (H_2O_2) and 2,5-diphenyloxazole (PPO).

efficiency of the chemiexcitation step in the presence of high water concentrations (70).

MECHANISTIC STUDIES ON THE PEROXYOXALATE SYSTEM IN AQUEOUS MEDIA

Many reports have been made, particularly recently (70–77), regarding the determination of the reaction mechanism of the peroxyoxalate chemiluminescence (PO-CL) transformation in aqueous environment. The determination of mechanisms relies

heavily on kinetic measurements and in the interpretation of molecularity made from observed reaction rates (78–80). The PO-CL system benefits from producing a signal that can be conveniently registered during a given time – *light* (7,15,22). Observed rate constants can then be obtained from the mathematical treatment of such CL-intensity *versus* time kinetic profiles (15), and relationships with reagents' concentrations and other parameters can be established from them. Although the amount of light, as given by the transformation's chemiluminescence quantum yield (Φ_{CL}), is usually orders of magnitude lower in aqueous environment compared to anhydrous organic solvents (15), light emission intensities are easily recorded with commercial fluorescence spectrophotometers and luminometers.

The aryl oxalate esters that are typically used for PO-CL studies in anhydrous media (15,18,37–43) are also applied in studies in aqueous environments, by far the most common one being bis (2,4,6-trichlorophenyl)oxalate (TCPO, Fig. 3) (70–77). Nonetheless, other oxalate derivatives with distinct reactivity have also been used (Fig. 3), either possessing electron-withdrawing substituents, for example, bis(4-nitrophenyl) oxalate (DNPO) (70), bis(3-(methoxycarbonyl)phenyl) oxalate (3MCPO) (71) and bis (2-(methoxycarbonyl)phenyl) oxalate (2MCPO) (72), as well as electron-donating groups, such as bis(4-methylphenyl) oxalate (MePO) (72, 77) and bis(4-methoxyphenyl) oxalate (MeOPO) (77) (Fig. 3).

In an earlier study of the PO-CL reaction in THF/water 5:2, using 0.025 mol L^{-1} potassium hydrogen phthalate buffer at pH = 4.0, Orosz studied sixteen different oxalate esters among symmetrical diaryl derivatives (*e.g.* TCPO, DNPO and diphenyl oxalate) and unsymmetrical phenyl aryl oxalates (81). The author explored the effect of the concentrations of oxalate ester, H_2O_2 and 9,10-bis(phenylethynyl)anthracene (BPEA, used as ACT), in order to rationalize the reaction mechanism, pointing out the importance of buffered systems in maintaining acid–base equilibria during the reaction of the oxalate ester with H_2O_2 (81).

By the time (62, 81–83), the formation of an oxalic peracid derivative (**OPD**) and 1,2-dioxetanedione (**3**) as reaction intermediates (Scheme 4) in aqueous media was envisioned, likewise to anhydrous systems, and hydrolysis of the oxalate ester was already pointed out (62,81) as a complex factor to be taken into account regarding mechanism determination (15). Indeed, CL-intensity time profiles were analyzed together with kinetic data for products formation (*i.e.* phenol and CO_2), obtained using gas chromatography (81) and IR absorption spectroscopy (82,83), in order to provide possible reaction pathways. Apart from considering the complete PO-CL transformation, studies aiming solely at the hydrolysis of oxalate esters in aqueous media also brought relevant insights (82,84,85). Using UV–Vis absorption spectroscopy the hydrolysis of DNPO in ACN/water mixtures of varying H_2O concentrations up to 2.78 mol L^{-1} (*i.e.* 5% v/v) was studied (85). With such a reactive oxalate ester, it has been proposed that the first ester group is hydrolyzed *via* the unorthodox $B_{AC}3$ mechanism, in which a water molecule acts as a general base assisting the addition of a second water molecule to the ester group (85). This generates a monoaryl oxalate intermediate that decomposes through decarboxylation and decarbonylation (85). The spontaneous decomposition of this intermediate was also proposed as final step in the hydrolysis of DNPO with $[H_2O]$ = 2.2 mol L^{-1} in THF (82). In the absence of water, with [MeOH] = 1.67 mol L^{-1} in ACN, solvolysis occurred by the consecutive substitution of the two phenolic groups of DNPO, with the first one being sixty times faster than the second (85).

With less reactive oxalate esters, possessing poorer leaving groups associated to the two carboxylate functionalities, it was observed that complete hydrolysis and/or solvolysis also takes place (62,84,86). As already stated, hydrolysis could be a major factor for the reduction of Φ_{CL} in aqueous environments compared to anhydrous ones (15), since the nucleophilic addition of water (or other polar protic solvent molecule) to the oxalate ester competes with the reaction with H_2O_2 to generate **ODP** (Scheme 4). Soares *et al*. observed that the solvolysis/hydrolysis of TCPO in EtOH/water and MeOH/water mixtures occurs with the production of the first phenolic residue with observed rate constants up to two orders of magnitude faster than the second one (86). Using the concept of solvent ionizing power (87–89) the authors concluded that in 100, 98 and 95% EtOH/water (% in v/v) a late transition state was involved in both consecutive steps, but this was not the case for mixtures with lower ionizing power (EtOH/water ≤90%; and 100 to 70% MeOH/water) (86). The observation of a solvent kinetic isotope effect going from inverse (in pure MeOH) to normal (in 70% MeOH/water) was additionally interpreted as resulting from general acid catalysis (86).

Neuvonen studied the neutral solvolysis of bis(4-nitrophenyloxalate) (4NPO) in ACN/water media with $[H_2O]$ ranging from 10.6 to 41.7 mol L^{-1}, comparing the obtained results with kinetic data for the hydrolysis of different highly reactive esters (84). Hydrolysis of the first phenolic residue in 4NPO is much faster than the second and occurs through a $B_{AC}3$ mechanism (84), as seen before for the hydrolysis of DNPO in ACN/water, the latter at a much lower $[H_2O]$, though (85). When 4NPO hydrolysis is catalyzed by imidazole (IMI-H), the two 4-nitrophenol residues are generated consecutively, giving rise to the 1,1′-oxalyldiimidazolide intermediate (ODI) (84). The unique reactivity of the 4NPO/IMI-H system in generating ODI was attributed to the stabilization of the transition state leading to its formation (84). In such transition state, the carbonyl group adjacent to the reaction center comprising the tetrahedral intermediate forms an intermolecular hydrogen-bonding network with IMI-H molecules, stabilizing the departure of the negatively charged phenolate group (84). The existence of ODI as intermediate can also rationalize the complex kinetic behavior observed for the PO-CL reaction of TCPO with H_2O_2, in the presence of 9,10-diphenylanthracene (DPA) as ACT and in 75% ACN/water IMI-H buffer (pH = 7.0) – although ODI was not explicitly mentioned by the authors. As it has been well-known for a while, ODI is a key intermediate for the standard PO-CL reaction in anhydrous media under IMI-H catalysis (15,63–67). Recently, it has been shown that IMI-H can catalyze the decomposition of **3** with an estimated bimolecular rate constant of 1.32×10^4 L mol^{-1} s^{-1} in EtOAc (90). This means that IMI-H is almost four times as efficient as DPA to catalyze the decomposition of the HEI (90), resulting in significantly lower Φ_{CL} values with increasing [IMI-H], as IHI-H can act only as "dark" catalyst, not an ACT with excited-state formation (66,67). In conditions optimized for high light emission quantum yields, with TCPO/H_2O_2/IMI-H and rubrene as ACT, the maximum obtained Φ_{CL} value in anhydrous medium was 6.7×10^{-1} E mol^{-1} (41), whereas, using other polycyclic aromatic hydrocarbons (HPAs) as ACTs, such as DPA and 2,5-diphenyloxazole (PPO) in the same conditions, the recorded maximum Φ_{CL}

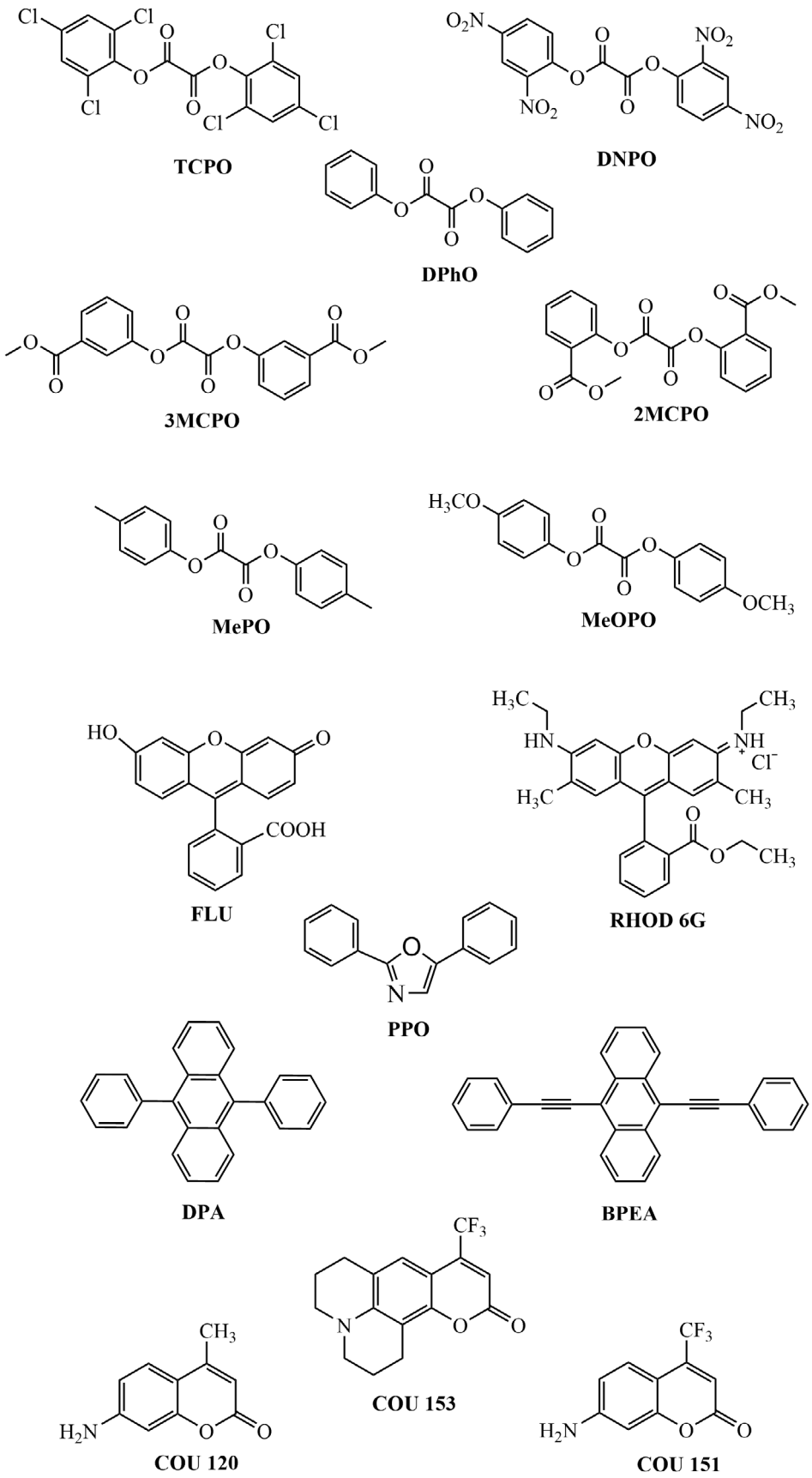

Figure 3. Molecular structures for the oxalate esters and activators used in studies of the PO-CL reaction in aqueous environments.

values were 5.7×10^{-2} and 9.1×10^{-4} E mol^{-1} (41), respectively.

In the search for alternative PO-CL catalysts for aqueous media, Souza *et al*. investigated the role of phosphate buffer on the kinetics of the reaction, using water mixtures with 1,2-dimethoxyethane (DME) as media (77). For the reaction of TCPO with H_2O_2 in DME/water 1:1 at pH = 8.0, with tetrabutylammonium phosphate (TBAP) buffer concentrations ranging from 12.5 to 100 mmol L^{-1}, the authors observed Φ_{CL} *ca.* 10^{-5} mol L^{-1} with PPO (77) – a value comparable to the one in anhydrous conditions, for the same ACT (Table 1). Kinetic evidence for both general acid and base catalysis was obtained and Φ_{CL} slightly decreased going from pH = 8.0 to 6.0. The use of MePO and MeOPO, oxalate esters containing poorer leaving groups, led to rates of perhydrolysis that were two orders of magnitude higher in comparison to hydrolysis (Table 1), an effect linked to an increased efficiency of general acid catalysis (Scheme 5) (77).

Using sodium salicylate (Sal) as base catalyst for the reaction of TCPO with H_2O_2 in anhydrous EtOAc, with DPA as ACT, it was observed that the transformation's rate determining step involves TCPO, H_2O_2 and Sal molecules simultaneously, in a highly ordered transition state, further confirmed through the determination of activation parameters (Scheme 5) (76). For this TCPO/H_2O_2/Sal system, shifting from EtOAc to DME/water 1:1, reduced Φ_{CL} by one order of magnitude, as well as promoted specific base catalysis (72). Specific base catalysis was also observed for MePO and 2MCPO, while the latter resulted in higher light yield generation (72). When the maximum singlet-excited state formation quantum yield (Φ_S) was investigated for the TCPO/H_2O_2/Sal system in DME/water 1:1, an increase in [Sal] promoted a systematic decrease in Φ_S (Table 1) (72). This was interpreted as decomposition of the HEI **3** by Sal (72), in a similar fashion to what happens in the TCPO/H_2O_2/IMI-H system (Scheme 5).

While Sal has been shown to promote specific base catalysis in DME/water 1:1, Augusto *et al*. demonstrated that the non-nucleophilic base 2,6-lutidine (Lut, a.k.a., 2,6-dimethylpyridine) can act as general base catalyst (74), obtaining kinetic data by CL-intensity time profiles and also registering the formation of 2,4,6-trichlorophenolate residues by UV–Vis absorption spectroscopy. For the TCPO/H_2O_2/Lut system in organic (pure DME) and water media, it was observed that both Lut and H_2O_2 are involved in the rate determining step of the reaction (Scheme 5) (74). By using a 20 mmol L^{-1} borate buffer, the concentration of Lut was changed while keeping the pH constant at 8.2, revealing a linear dependence of the observed rate constant with base concentration, ultimately suggesting general base catalysis (74). The determined termolecular rate constants for the reaction in DME and water were, respectively, 1.8 and 26 L^2 mol^{-2} s^{-1} (Table 1); the development of charge during the transition state of the Lut catalyzed H_2O_2 attack to the ester functionality is better stabilized in the more polar medium, justifying the increased rate constant value in water (Scheme 5) (74).

The PO-CL reaction of TCPO/H_2O_2/Lut in water, using fluorescein as ACT, showed Φ_{CL} values of up to 5×10^{-5} E mol^{-1}, while this yield was only slightly higher in pure DME (74). When ionic liquids (ILs) were used with the TCPO/H_2O_2 system

Table 1. Compilation of kinetic and quantum yield data for peroxyoxalate systems studied in aqueous media.

Media	Oxalate ester	Catalyst	Catalysis type	k_{hyd} (s^{-1})*	$k_{per}[H_2O_2]$ (s^{-1})†	ACT	Φ_S (E mol^{-1})‡	Ref.
DME/water, $[H_2O]$ = 0.7 mol L^{-1} DME/water 1:1	TCPO	IMI-H	Nuc, GBC	7.3×10^{-4}	2.2×10^{-4}	DPA	4.6×10^{-3}	(70)
	DNPO		GBC	2.7×10^{-3}	6.3×10^{-2}		3.0×10^{-3}	
	TCPO					COU153	1.9×10^{-3}	(71)
						COU120	1.4×10^{-4}	
						COU151	1.5×10^{-4}	
	3MCPO		§	§	§	COU153	2.8×10^{-4}	
						COU120	1.3×10^{-5}	
						COU151	2.0×10^{-5}	
	TCPO	Salicylate	SBC	2.27×10^{-5}	2.92×10^{-3}	Rhodamine 6G	5.7×10^{-3}	(72)
	MePO			2.14×10^{-5}	1.67×10^{-3}		5.9×10^{-8}	
	2MCPO			*irrelevant*	7.80×10^{-3}		7.5×10^{-4}	
Carbonate buffer (pH = 10.4)	TCPO	Carbonate		7.3×10^{-1}	2.5×10^{0}	Fluorescein	5.8×10^{-7}	(73)
Borate buffer (pH = 8.2)		2,6-Lutidine	GBC	8.0×10^{-2}	1.51×10^{-2}		8.8×10^{-5}	(74)
Borate buffer (pH = 9.2, with 20% ionic liquid)		$BMIBF_4$	SBC	1.2×10^{-1}	1.8×10^{-1}	Rhodamine 6G	4.1×10^{-4}	(75)
		AMICl		3.0×10^{-3}	9.8×10^{-2}		1.4×10^{-4}	
		AMIAc		5.1×10^{-2}	1.2×10^{-2}		1.1×10^{-4}	
DME/water 1:1 (phosphate buffer, pH = 7.0)	TCPO	Phosphate	GAC, GBC	4.0×10^{-1}	1.2×10^{-1}	PPO	1.4×10^{-5}	(77)
	MePO			1.6×10^{-1}	2.0×10^{-1}		4.2×10^{-7}	
	MeOPO			2.0×10^{-2}	3.4×10^{-1}		2.5×10^{-8}	

Nuc = nucleophilic; GAC = general acid catalysis; GBC = general base catalysis; SBC = specific base catalysis. *For the highest observed Φ_S at a given aqueous condition. †For the highest observed Φ_S at a given aqueous condition, with $[H_2O_2]$ = 10.0 mmol L^{-1}. ‡Highest value observed at a given aqueous condition. §The parameter was not formally discussed in the cited report.

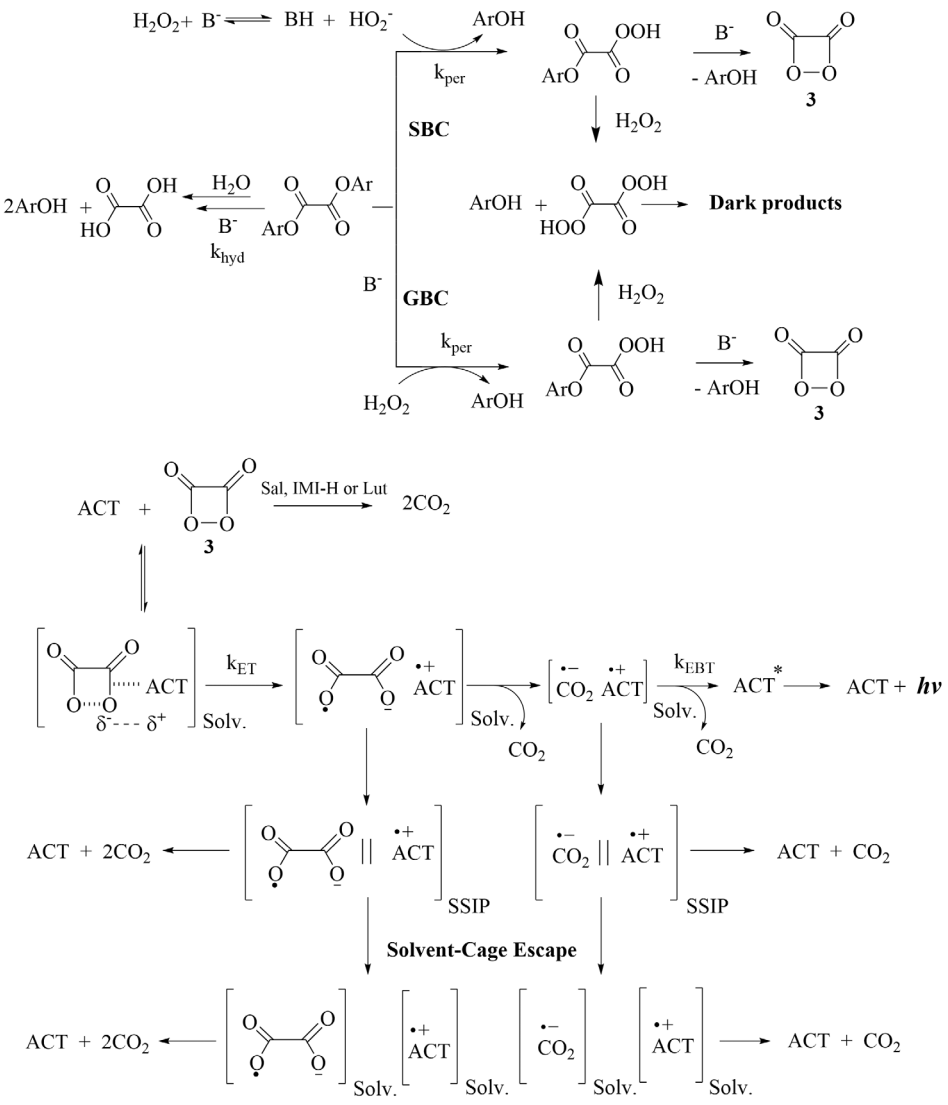

Scheme 5. Reaction pathways for the peroxyoxalate system in aqueous medium, in the presence of base (B_ catalysts; SBC, Specific Base Catalysis; GBC, General Base Catalysis; ACT, activator; IMI-H, imidazole; Sal, sodium salicylate; Lut, lutidine; k_{ET}, electron transfer rate constant; k_{EBT}, electron back-transfer rate constant; solv., solvated ion pairs or ions; SSIP, solvent-separated ion pairs.

in 50 mmol L^{-1} borate buffer (pH = 8.2), using rhodamine 6G as ACT, it was observed that the increase in ILs concentration led to a suppression of the hydrolysis reaction, increasing Φ_S values (75). It was shown that the observed rate constants depend on $[H_2O_2]$ but not on borate buffer concentration, indicating specific base catalysis and that TCPO reacts directly with the hydroperoxide anion HOO^- within the reaction sequence that leads to the HEI **3** (Scheme 5) (75). Increase in Φ_S from 10^{-5} up to 10^{-4} E mol^{-1} was observed for three imidazole-based ILs, 1-butyl-3-methylimidazolium tetrafluoroborate ($BMIBF_4$), 1-allyl-3-methylimidazolium chloride (AMICl) and 1-allyl-3-methylimidazolium acetate (AMIAc), in comparison to the aqueous buffer solution without ILs (Table 1) (75). When simple electrolytes (*i.e.* NaCl, tetrabutylammonium tetrafluoroborate and acetate) were used, increase in their concentration promoted increased reaction rates and lowered Φ_S compared to the media containing only the borate buffer (75). Correlations between Φ_S values and the viscosity and empirical polarities of the ILs/aqueous borate buffer solutions revealed that medium polarity, and not viscosity, is the key factor for determining the magnitude of the chemiexcitation yield, Φ_S (75). At the observed optimal polarity of E_T (33) *ca.* 67 kcal mol^{-1}, the environment is able to stabilize the formation of the radical-ion pair of the CIEEL sequence, but polarity is not high enough as to promote escape from the solvent cavity and separation of the charged species (Scheme 5) (75).

Hydroperoxide anion HOO^- is the nucleophilic species reacting with TCPO in aqueous borate buffer (75) as well as in carbonate buffer (73). For the TCPO/H_2O_2 system, using fluorescein as ACT, observed rate constants increased one order of magnitude from pH = 9.4 to 11.2, while also depending on $[H_2O_2]$ and remaining unchanged within a wide variation in the carbonate buffer concentration (0.02 to 0.15 mol L^{-1}), thus, suggesting specific base catalysis (Scheme 5) (73). Although in completely aqueous carbonate buffer, the reaction is fast and convenient for possible analytical applications, the maximum observed Φ_S was 10^{-7} E mol^{-1} (73), much lower than the 10^{-5} E mol^{-1} obtained with other, however partial, aqueous environments (Table 1)

(72,74,75,77). This low chemiexcitation yield could be attributed to the extensive hydrolysis of the oxalate ester, since it has been determined that the bimolecular rate constants associated with hydrolysis and perhydrolysis in carbonate buffer are both *ca.* 4×10^3 L mol^{-1} s^{-1} (73); taking into account the concentration of water of the aqueous media, hydrolysis is prominently consuming the oxalate ester. Increasing [H_2O_2] does increase Φ_S but only until a certain point, beyond which the formation of bis-peroxalate anion is largely responsible for reducing the quantum yields of chemiexcitation (Scheme 5) (73–75).

Hydrolysis has been pointed out as the major responsible for reducing the Φ_S values of the PO-CL reaction in aqueous media when compared to anhydrous ones. Nevertheless, this view cannot longer be sustained. Even in extremely alkaline conditions as in carbonate buffer, Φ_S is too low to be explained solely by occurrence of oxalate ester hydrolysis (73). As stated above and supported in many accounts (70–72,75,77), the reduced Φ_S in aqueous media is more likely to be related to the low efficiency of the chemiexcitation step for high polarity media. It was observed for the TCPO/H_2O_2/IMI-H and DNPO/H_2O_2 systems in DME/water mixtures, going from pure organic solvents to [H_2O] up to 7 mol L^{-1}, that in higher water concentrations H_2O_2 reacts directly with TCPO without involvement of nucleophilic IMI-H catalysis, whereas no nucleophilic IMI-H catalysis appears to operate for DNPO, even in anhydrous conditions (70). For both TCPO and DNPO in DME/water mixtures, the recorded perhydrolysis rate constants are several orders of magnitude higher than the corresponding hydrolysis rate constants (Scheme 5) (70). Additionally, it was observed that with both esters Φ_S values increased up to [H_2O] = 0.7 mol L^{-1}, reaching chemiexcitation yields as high as 5×10^{-3} E mol^{-1} (Table 1), decreasing afterwards for superior water concentrations (70); constituting the first report of a systematic increase in Φ_S with water concentration for the PO-CL reaction. It was hypothesized that the chemiexcitation efficiency may be related to a solvation effect involved with the bimolecular interaction between the HEI and ACT, within the CIEEL sequence (70). This may occur due to a medium polarity effect, or even due to a specific molecular water effect that could stabilize the generated radical-ion pair through hydrogen-bonding (Scheme 5) (70). As it turns out, while a lot of water may reduce chemiexcitation efficiency, the right amount is likely beneficial to the generation of charged species involved with electron transfer and bond breaking.

Finally, there is a continuous search for molecules that could serve as proper ACTs for the PO-CL transformation, possessing low oxidation potentials (*i.e.* <1.2 V *vs* SCE) and high fluorescence quantum yields (ideally above 10%) (15). As most ACTs are HPAs or direct derivatives from such hydrocarbons these are unsuitable for use in aqueous media, mainly due to solubility concerns. Possible alternatives to HPAs that have been used as ACTs for PO-CL in water are fluorescein (73–75) and rhodamine 6G (72,75), while PPO can be also applied with aqueous mixtures with miscible organic solvents (77), as it is a much more polar substance compared to anthracene derivatives. Although there is a huge number of reports regarding the use of new possible ACTs, even in aqueous media, few works are concerned with understanding the process by which singlet-excited states are generated (42,71,91). One recent report by Cabello, Bello and Baader promoted the use of three coumarin derivatives, COU120, COU151 and COU153 as greener ACT alternatives for the PO-CL reaction (71). All three coumarins presented maximum Φ_S values similar to the ones of typical HPAs, in both DME and DME/water 1:1 media, while evidence for the occurrence of an electron transfer (or at least charge transfer) during chemiexcitation was also obtained (71). The authors also compared the quantum efficiency of the environmentally compatible 3MCPO with the one for TCPO, finding out that both oxalate esters have equivalent chemiexcitation yields and that for 3MCPO in DME/water 1:1 Φ_S is only five-times smaller compared to pure DME (Table 1) (71).

In summary, the mechanistic studies of peroxyoxalate CL in aqueous media revealed that, depending on the experimental conditions, hydrolysis (no light emission) or perhydrolysis (with light emission) can be predominant using a common hydrogen peroxide concentration of 10.0 mmol L^{-1}. Hydrolysis is predominant with lutidine, whereas with imidazole, ionic liquids and phosphate buffer, both processes occur generally to a similar extent. Using salicylate as catalyst, perhydrolysis occurs predominantly with TCPO, MePO and 2MCPO as oxalic esters, with perhydrolysis rate constants two orders of magnitude higher than hydrolysis (Table 1). Whereas, with carbonate buffer perhydrolysis is three times faster than hydrolysis. Using the ionic liquid AMICl and TCPO as ester, perhydrolysis overcomes hydrolysis in one order of magnitude; similar to the situation with phosphate catalysis for the ester MeOPO, for which perhydrolysis is 10 times faster than the hydrolysis. The determined quantum yields in the utilized aqueous media span a wide range, from 3×10^{-8} to 5×10^{-3} E mol^{-1} – or, simply, 0.000003 to 0.5% – using different oxalic esters and activators. The highest yields of up to 0.5% are obtained with TCPO and DNPO in DME containing 0.7 mol L^{-1} H_2O with DPA as ACT. Whereas in DME/water 1:1 and TCPO with coumarins as ACTs yields are 0.02 to 0.2%; with 3MCPO as ACT yields are one order of magnitude lower (Table 1). With TCPO as ester, ROD6G as ACT in DME/water 1:1 yields of up to 0.6% are obtained, whereas with ionic liquids and Lut as catalysts and ROD6G and fluorescein as ACTs, quantum yields are in the 0.01% range. The lowest quantum yields are reported for phosphate catalysis; however, in this case, the low-efficient activator PPO has been utilized (Table 1).

APPLICATIONS OF PO-CL

Since the first practical application of the peroxyoxalate system (PO-CL), the production of a "light stick" (92), the reaction has found a wide range of analytical and bioanalytical applications due to its high quantum yields and the possibility of CL emission in all the visible spectrum, also ranging to UV and near-infrared (NIR) emission (93). On the other hand, as mentioned before, the most important limitation of this reaction is its sensitivity to water, primary alcohols and other nucleophilic solvents, which can attack and degrade the oxalic ester negatively affecting the chemiluminescent emission. Furthermore, both peroxyoxalate and fluorophores are generally insoluble in water, which is another factor that also limits their applications in aqueous systems.

There has been a wide range of established methods for encapsulating PO-CL systems in recent years. The inclusion of ester and an activator in organized systems increases the local concentration of these components. It shortens the distance between the donor and the acceptor, which improves the efficiency of chemiluminescence resonance energy transfer (CRET)

(94). Moreover, the use of these ideal media favors perhydrolysis, the peroxide attack on the oxalic ester, which leads to a greater formation of the HEI and consequently a more significant chemiluminescent emission. Herein, we will highlight a selection of the most recent analytical and bioanalytical applications of the peroxyoxalate system in aqueous media.

Analytical applications

Quantum Dots (QDs) have been widely used in several fields due to their many advantages, such as their high quantum efficiency, excellent water solubility, *etc*. (95,96). Cai *et al*., studied the peroxyoxalate system containing Graphene Oxide Quantum Dots (GOQD) and fluorescein applied to determine 4-nitrophenol (4-NP), considered to cause a high environmental impact due to its toxicity and persistence, in enriched tap water and river water (97). In this report it was observed that the CL intensity increased with the addition of 4-NP into the TCPO-H_2O_2-fluorescein-GOQD system. Based on these facts it was speculated that the hydroxyl and nitro groups of the 4-NP molecule combine with the carboxyl and hydroxyl groups on GOQD through hydrogen bonding, and the steric configuration of the 4-NP molecule contributes to the interaction with the GOQD. This interaction will promote the energy transfer process from GOQD to fluorescein and increase the CL emission (97).

On the other hand, using bis-(2,4,6-trichlorophenyl) oxalate (TCPO) as oxalic ester, the PO-CL was also utilized to detect phloroglucinol in environmental water samples using glutathione-coated cadmium telluride quantum dots (GSH-CdTe QDs) instead of conventional fluorophores (98). In this case, contrarily mentioned in the above example, the CL intensity was reduced with the addition of analyte phloroglucinol. UV–vis absorption spectra demonstrated that this analyte reacted with H_2O_2 and decreased the formation of excited-state QDs; therefore, the CL emission is inhibited (98).

Another practical application of the PO system is using it to determine micellar transitions in a variety of surfactant solutions (99). Including peroxyoxalate reagents and fluorophores in hydrophobic cavities constitutes a promising strategy for the nondestructive characterization of micelles in solution. In addition, other studies have shown that the use of anionic and nonionic surfactants in micellar media increases the efficiency of the reaction of TCPO with H_2O_2 using oligophenylenevinylene as activators (100). PO-CL is also commonly applied in food analysis, where molecularly imprinted polymers (MIP) are used to reconstitute nonanalyte substances, which increase CL emission. Li *et al*. first developed this method to determine ethopabate residues in chicken muscle (101), which has also been used for the detection of Sudan dyes in egg (102). In both cases, the analytes were quantified using the TCPO-H_2O_2-IMI-H system. In general, the polymers were immobilized in a 96-well microplate, and through the optimization of the MIP absorption and CL imaging conditions, a linear relationship was obtained between the relative CL intensity and the concentrations of the analytes (101,102).

The PO-CL system has also been used to determine the antioxidant activity of compounds in edible oils (103) and residual pesticides in food and water (104–107). In these prior studies the system was utilized with TCPO or bis[2,4,5-trichloro-6-(pentyloxycarbonyl)phenyl] oxalate (CPPO) as a peroxyoxalate derivative, H_2O_2 and rubrene or gold nanoparticles as acceptors to harvest the energy *via* CRET process and the pesticide detected and quantified through their quenching effect on CL emission. The PO-CL reaction was also utilized to detect traces of methamphetamine-based compounds in mouse hair roots, halofantrine (an anthracene-methanol derivative used in malaria treatment) in mouse plasma (108), catecholamines in mouse brain samples (109) and in human plasma (110), among many other applications.

Bioanalytical applications

The peroxyoxalate system can also be applied in different fields of pharmacology and diagnosis. Because malignant cells produce increased amounts of hydrogen peroxide, oxalate-based formulations can be used to show foci of tumor growth and other inflammatory processes. Previously, Dasari *et al*. (111) developed chemiluminescent micelles composed of poly(ethylene glycol)-b-poly(ε-caprolactone) (PEG-PCL) copolymer and diphenyl oxalate, which is more stable in water than TCPO. Diphenyl oxalate was encapsulated in the hydrophobic nuclei and, therefore, protected from hydrolysis by water, increasing its stability. Subsequent studies demonstrated that these microenvironments composed of diphenyl oxalate could be used to detect hydrogen peroxide generated from activated macrophages by lipopolysaccharide (LPS) (112). Therefore, in general, PO-CL micelles have great potential in biological applications due to their ability to detect nanomolar concentrations of hydrogen peroxide (111–116). One of the most recent applications for this system has been the formulation of peroxyoxalate liposomes composed of TCPO and curcumin as a fluorophore, capable of detecting H_2O_2 and serving as therapeutic agents with antioxidant activity and potent anti-apoptotic (117).

Meanwhile, a limitation of the PO system for *in vivo* bioimaging and biosensor applications is that the direct chemiluminescence resonance energy transfer (CRET) process can only be operated in the 400–850 nm range. The emission in this wavelength region is readily absorbed and scattered by the molecules and cells in biological matrices (118), limiting the high-performance of *in vivo imaging*. In recent years, several researchers have introduced some methods to extend the wavelength emission by introducing Förster resonance energy transfer (FRET) processes after the CRET process (119). The CL substrate is oxidized by H_2O_2, forming the 1,2-dioxetanedione intermediate, which transfers chemical energy to a fluorescent dye through the CRET process. Subsequently, this fluorophore transfers energy to another dye through FRET to provide CL signals in longer wavelengths. In this sense, Mao *et al*. developed chemiluminescent nanoparticles (NPs) encapsulating CPPO and thiadiazole-2-(diphenyl methylene) malononitrile (TBD) photosensitizer in a pluronic polymer F-17 using soybean oil as a retardant for image-guided tumor therapy (120). In this study, the resulting NPs exhibited intense far-red (FR) / near-infrared (NIR) chemiluminescence, which are advantageous emission wavelengths for bioimaging due to better tissue penetration. Additionally, the NPs showed a strong ability to generate $^1O_2$ in the presence of H_2O_2, proofing to be of potential therapeutic utility. Another recent promising application was the development of a chemiluminescent sensor in the Second Infrared Region that can be selectively activated by H_2O_2 over other reactive oxygen species, and with a penetration depth of ~8 mm for high-contrast imaging of *in-vivo* inflammation (121). Nanosensors based on the PO reaction were also developed for fast and real-time

in vivo imaging of drug-induced reactive oxygen species (ROS) and reactive nitrogen species (RNS) for direct evaluation of hepatotoxicity (122).

Another application of the PO system is the development of CL Nanoprobes called "biolighted luminescent nanotorch (BioNT)" that perform the precise identification of inflammation by systemic self-delivery to pathological tissues (123). In this sense, nanoparticles were prepared by encapsulating CPPO and an anthracene-cored hydrophobic dye (BDSA) in a polymeric surfactant, Pluronic F-127. BDSA was employed as an emitting component for PO-CL, whose chromophoric unit has been reported to show strong reddish solid-state fluorescence (SSF) in the nanoaggregated forms. BioNT colloidal size was small enough for long systemic circulation, and the emission spectrum covered the tissue-penetrating near-infrared (NIR) region (>650 nm), being advantageous for *in vivo* imaging. Upon subcutaneous injection to a normal mouse, BioNT displayed light emission throughout the whole body, initiated by endogenous H_2O_2. Furthermore, it was observed that the nanoprobes were accumulated in pathological tissues where the CL intensity reflects the level of H_2O_2 abnormally overproduced by inflammation and that BioNT exhibits no apparent toxicity, thus holding potential for high-contrast diagnostic imaging (123).

On the other hand, the reaction of TCPO, H_2O_2 and safranin O as the fluorophore, catalyzed by silver nanoparticles, demonstrated its effectiveness for the determination of 6-mercaptopurine (6-MP) in commercial pharmaceutical samples, an immunosuppressive drug used to treat leukemia (124). In this work, the formation of $OH^{\cdot}$ radical by the catalytic action of silver nanoparticles to H_2O_2 has been shown. This unstable reactive intermediate could attack H_2O_2 to generate a superoxide anion, which accelerates the production of 1,2-dioxetanedione, thus strongly increasing the CL signal. Based on this reaction mechanism, this method was developed to assay the presence of 6-MP due to the inhibition effect of this analyte on the PO-CL system. In this sense, it was supposed that the reducing groups of, NH_2, or SH are likely to compete with TCPO for active oxygen intermediates, leading to a decrease in CL intensity (124).

Chemiluminescent semiconductor polymeric nanoparticles (SPNs) have also been developed and optimized for ultrasensitive *in vivo* imaging of H_2O_2 (125). More recently, Li *et al*. demonstrated that nanoparticles involving CPPO, rubrene and alginate hydrogel doped with glucose oxidase could detect and image the local concentration of glucose at the periphery of the tumor (126). Other nanoparticles of CPPO and Hypocrellin B (CBNPs) for Ultrasound-Enhanced Self-Exciting Photodynamic Therapy also showed an excellent therapeutic effect against cancer cells (127). In this last paper, relevant *in vitro* experiments against cancer cells were performed. Under stimulation of ultrasound (US) and the presence of H_2O_2 it was observed that nanoparticles exhibited more efficient $^1O_2$ generation ability, which induces cell apoptosis. Measurements of cell viability demonstrated that CBNPs significantly inhibited the growth of cancer cells, providing a novel strategy for improving Photodynamic Therapy efficiency (127).

QDs in the peroxyoxalate reaction under physiological conditions have also proved promising for biological analysis and especially suitable for *in vivo* biosensors (128). In this study, the chemiluminescence quantum yields were about 200 times higher than that of the more commonly used luminol system. Lippert *et al*. developed a chemiluminescence assay and device, based on the PO reaction, to measure nanomolar concentrations of hydrogen peroxide in the condensate of exhaled air from asthma patients and healthy participants (129).

In summary, several studies of applications of the peroxyoxalate reaction were carried out in different microenvironments in order to increase the low efficiency of the reaction observed in aqueous media and improve its analytical sensitivity.

CONCLUSIONS

The unimolecular decomposition of cyclic peroxides like 1,2-dioxetanes and 1,2-dioxetanones leads to the preferential formation of nonemissive triplet-excited species, therefore, not constituting an adequate model for efficient BL and CL transformations.

Catalyzed decomposition of certain peroxides can lead to preferential singlet-excited state formation, necessary for efficient BL and CL; however, the so-called intermolecular CIEEL showed to be of low efficiency, except for the peroxyoxalate reaction, where interaction of the high-energy intermediate formed in the transformation with an appropriate activator leads to efficient singlet-excited state formation and high CL emission.

The intramolecular version of CIEEL – induced decomposition of phenoxy-substituted 1,2-dioxetane derivatives – leads to highly efficient singlet chemiexcitation and high CL emission, constituting a chemical model for efficient BL.

The high efficiency of the peroxyoxalate reaction in anhydrous media drops down significantly when performed in aqueous media, as also observed for other CL transformations.

Mechanistic studies on the peroxyoxalate reaction in diverse aqueous media show that reproducible kinetics can be performed in these conditions. The thermal reactions for the formation of the high-energy intermediate – 1,2-dioxetanedione – can occur by specific and general base catalysis.

Whereas the emission quantum yields are generally several orders of magnitude lower in aqueous media than in anhydrous solvents, optimal conditions can be found in which these yields are similar, specifically in organized media.

The generally lower quantum yields in aqueous media are not only due to the hydrolysis of the used oxalic ester derivatives, but also appear to be caused by a reduction of the chemiexcitation efficiency in the presence of high amounts of water.

Interestingly, low water concentrations (below 1 mol L^{-1}) can lead to an increase in the chemiexcitation efficiency, probably due to the stabilization of ion pairs formed in the chemiexcitation step by solvation.

Several examples of the utilization of the peroxyoxalate reaction in analytical and bioanalytical applications show that even being less efficient in aqueous media the PO-CL reaction can be utilized to detect various analytes.

Acknowledgements—The authors thank the Fundação de Amparo à Pesquisa do Estado de São Paulo (FAPESP, WJB 2014/22136-4; FHB2012/13807-7, 2022/02183-4), Conselho Nacional de Desenvolvimento Científico e Tecnológico (CNPq, productivity fellowship 303015/2019-5 for W.J.B., PhD fellowships for MCC, 147138/2016-7) and Coordenadoria de Aperfeiçoamento de Pessoal de Ensino Superior (CAPES, Graduate Program of Chemistry, IQUSP (Finance Code 001)) for financial support.

REFERENCES

1. Vacher, M., I. Galván, B.-W. Ding, S. Schramm, R. Berraud-Pache, P. Naumov, N. Ferré, Y.-J. Liu, I. Navizet, D. Roca-Sanjuán, W. J. Baader and R. Lindh (2018) Chemi- and bioluminescence of cyclic peroxides. *Chem. Rev.* **118**, 6927–6974. https://doi.org/10.1021/acs.chemrev.7b00649
2. Lee, J. (2017) Perspectives on bioluminescence mechanisms. *Photochem. Photobiol.* **93**, 389–404. https://doi.org/10.1111/php.12650
3. Radziszewski, B. R. (1877) Untersuchungen über Hydrobenzamid, Amarin und Lophin. *Berichte der Dtsch. Chem. Gesellschaft* **10**, 70–75. https://doi.org/10.1002/cber.18770100122
4. Albrecht, H. O. (1928) Über die Chemiluminescenz des Aminophthalsäurehydrazids. *Phys. Chem.* **136**, 321–330. https://doi.org/10.1515/zpch-1928-13625
5. Gleu, K. and W. Petsch (1935) Die chemiluminescenz der dimethyl-diacridyliumsalze. *Angew. Chemie* **48**, 57–59. https://doi.org/10.1002/ange.19350480302
6. Chandross, E. A. (1963) A new chemiluminescent system. *Tetrahedron Lett.* **12**, 761–765. https://doi.org/10.1016/S0040-4039(01)90712-9
7. Rauhut, M. M. (1969) Chemiluminescence from concerted peroxide decomposition reactions. *Acc. Chem. Res.* **2**, 80–87. https://doi.org/10.1021/ar50015a003
8. Bastos, E. L., P. Farahani, E. J. H. Bechara and W. J. Baader (2017) Four-membered cyclic peroxides: Carriers of chemical energy. *J. Phys. Org. Chem.* **30**, 1–18. https://doi.org/10.1002/poc.3725
9. Kagalwala, H. N., R. T. Reeves and A. R. Lippert (2022) Chemiluminescent spiroadamantane-1,2-dioxetanes: Recent advances in molecular imaging and biomarker detection. *Curr. Opin. Chem. Biol.* **68**, 102134. https://doi.org/10.1016/J.CBPA.2022.102134
10. Adam, W. and J.-C. Liu (1972) Cyclic peroxides. XVI. Alpha-peroxy lactone. Synthesis and chemiluminescence. *J. Am. Chem. Soc.* **94**, 2894–2895. https://doi.org/10.1021/ja00763a077
11. Adam, W. and G. Cilento (1982) Chemical and biological generation of excited states. In *Chemistry*. https://doi.org/10.1016/b978-0-12-044080-1.x5001-9
12. Adam, W. and A. V. Trofimov (2006). In *The Chemistry of Peroxides*, Vol. **2** (Edited by Z. Rappoport), pp. 1171–1209. Wiley, New York.
13. Adam, W. and W. J. Baader (1984) 1,2-dioxetane: Synthesis, characterization, stability, and chemiluminescence. *Angew. Chem. Int. Ed. Engl.* **23**, 166–167. https://doi.org/10.1002/anie.198401661
14. Bartoloni, F. H., M. A. De Oliveira, F. A. Augusto, L. F. M. L. Ciscato, E. L. Bastos and W. J. Baader (2012) Synthesis of unstable cyclic peroxides for chemiluminescence studies. *J. Braz. Chem. Soc.* **23**, 2093–2103. https://doi.org/10.1590/S0103-50532012001100018
15. Ciscato, L. F. M. L., F. A. Augusto, D. Weiss, F. H. Bartoloni, S. Albrecht, H. Brandl, T. Zimmermann and W. J. Baader (2012) The chemiluminescent peroxyoxalate system: State of the art almost 50 years from its discovery. *ARKIVOC* **2012**, 391–430. https://doi.org/10.3998/ark.5550190.0013.328
16. Bos, R., S. A. Tonkin, G. R. Hanson, C. M. Hindson, K. F. Lim and N. W. Barnett (2009) In search of a chemiluminescence 1,4-dioxy biradical. *J. Am. Chem. Soc.* **131**, 2770–2771. https://doi.org/10.1021/ja808401p
17. Tonkin, S. A., R. Bos, G. A. Dyson, K. F. Lim, R. A. Russell, S. P. Watson, C. M. Hindson and N. W. Barnett (2008) Studies on the mechanism of the peroxyoxalate chemiluminescence reaction. Part 2. Further identification of intermediates using 2D EXSY13C nuclear magnetic resonance spectroscopy. *Anal. Chim. Acta* **614**, 173–181. https://doi.org/10.1016/j.aca.2008.03.009
18. Stevani, C. V. and W. J. Baader (1997) Kinetic studies on the chemiluminescent decomposition of an isolated intermediate in the peroxyoxalate reaction. *J. Phys. Org. Chem.* **10**, 593–599. https://doi.org/10.1002/(SICI)1099-1395(199708)10:8<593::AID-POC926>3.0.CO;2-H
19. Stevani, C. V., I. P. D. A. Campos and W. J. Baader (1996) Synthesis and characterisation of an intermediate in the peroxyoxalate chemiluminescence: 4-chlorophenyl O,O-hydrogen monoperoxyoxalate. *J. Chem. Soc. Perkin Trans.* **2**, 1645–1648. https://doi.org/10.1039/P29960001645
20. Farahani, P. and W. J. Baader (2017) Unimolecular decomposition mechanism of 1,2-dioxetanedione: Concerted or biradical? That is the question! *J. Phys. Chem. A* **121**, 1189–1194. https://doi.org/10.1021/acs.jpca.6b10365
21. da Silva, S. M., A. P. Lang, A. P. F. dos Santos, M. C. Cabello, L. F. M. L. Ciscato, F. H. Bartoloni, E. L. Bastos and W. J. Baader (2021) Cyclic peroxidic carbon dioxide dimer fuels Peroxyoxalate chemiluminescence. *J. Org. Chem.* **86**, 11434–11441. https://doi.org/10.1021/acs.joc.1c00929
22. Baader, W. J., C. V. Stevani and E. L. Bastos (2006) Chemiluminescence of organic peroxides. In *The Chemistry of Peroxides* (Edited by Z. Rappoport), pp. 1211–1278. Wiley-VCH, Chichester.
23. Turro, N. J. and A. Devaquet (1975) Chemiexcitation mechanisms. The role of symmetry and spin–orbit coupling in diradicals. *J. Am. Chem. Soc.* **97**, 3859–3862. https://doi.org/10.1021/ja00846a075
24. Adam, W. and K. Zinner (1982) Determination of activation parameters and the thermal stability of 1,2-dioxetanes. In *Chemical and Biological Generation of Excited States* (Edited by W. Adam and G. Cilento), pp. 153–189. Academic Press, New York. https://doi.org/10.1016/b978-0-12-044080-1.50010-9
25. Bastos, E. L. and W. J. Baader (2007) Theoretical studies on thermal stability of alkyl-substituted. *ARKIVOC* **2007**, 257–272. https://doi.org/10.3998/ark.5550190.0008.820
26. Adam, W. and W. J. Baader (1985) Effects of methylation on the thermal stability and chemiluminescence properties of 1,2-dioxetanes. *J. Am. Chem. Soc.* **107**, 410–416. https://doi.org/10.1021/ja00288a022
27. Schuster, G. B. (1979) Chemiluminescence of organic peroxides. Conversion of ground-state reactants to excited-state products by the chemically initiated electron-exchange luminescence mechanism. *Acc. Chem. Res.* **12**, 366–373. https://doi.org/10.1021/ar50142a003
28. Adam, W., G. A. Simpson and F. Yany (1974) Mechanism of direct and rubrene enhanced chemiluminescence during α-peroxylactone decarboxylation. *J. Phys. Chem.* **78**, 2559–2569. https://doi.org/10.1021/j100618a007
29. Koo, J. and G. B. Schuster (1978) Chemiluminescence of Diphenoyl peroxide. Chemically initiated electron exchange luminescence. A new general mechanism for chemical production of electronically excited states. *J. Am. Chem. Soc.* **100**, 4496–4503. https://doi.org/10.1021/ja00482a030
30. Koo, J. A., S. P. Schmidt and G. B. Schuster (1978) Bioluminescence of the firefly: Key steps in the formation of the electronically excited state for model systems. *Proc. Natl. Acad. Sci.* **75**, 30–33. https://doi.org/10.1073/pnas.75.1.30
31. Wilson, T. (1995) Comments on the mechanisms of chemi- and bioluminescence. *Photochem. Photobiol.* **62**, 601–606. https://doi.org/10.1111/j.1751-1097.1995.tb08706.x
32. Isobe, H., Y. Takano, M. Okumura, S. Kuramitsu and K. Yamaguchi (2005) Mechanistic insights in charge-transfer-induced luminescence of 1,2-dioxetanones with a substituent of low oxidation potential. *J. Am. Chem. Soc.* **127**, 8667–8679. https://doi.org/10.1021/ja043295f
33. Takano, Y., T. Tsunesada, H. Isobe, Y. Yoshioka, K. Yamaguchi and I. Saito (1999) Theoretical studies of decomposition reactions of dioxetane, dioxetanone, and related species. CT induced luminescence mechanism revisited. *Bull. Chem. Soc. Jpn.* **72**, 213–225. https://doi.org/10.1246/bcsj.72.213
34. Almeida De Oliveira, M., F. H. Bartoloni, F. A. Augusto, L. F. M. L. Ciscato, E. L. Bastos and W. J. Baader (2012) Revision of singlet quantum yields in the catalyzed decomposition of cyclic peroxides. *J. Org. Chem.* **77**, 10537–10544. https://doi.org/10.1021/jo301309v
35. Augusto, F. A., A. Francés-Monerris, I. Fdez Galván, D. Roca-Sanjuán, E. L. Bastos, W. J. Baader and R. Lindh (2017) Mechanism of activated chemiluminescence of cyclic peroxides: 1,2-dioxetanes and 1,2-dioxetanones. *Phys. Chem. Chem. Phys.* **19**, 3955–3962. https://doi.org/10.1039/c6cp08154a
36. Bartoloni, F. H., M. A. De Oliveira, L. F. M. L. Ciscato, F. A. Augusto, E. L. Bastos and W. J. Baader (2015) Chemiluminescence efficiency of catalyzed 1,2-dioxetanone decomposition determined by steric effects. *J. Org. Chem.* **80**, 3745–3751. https://doi.org/10.1021/acs.joc.5b00515

37. Khalid, M., S. P. Souza, L. F. M. L. Ciscato, F. H. Bartoloni and W. J. Baader (2015) Solvent viscosity influence on the chemiexcitation efficiency of inter and intramolecular chemiluminescence systems. *Photochem. Photobiol. Sci.* **14**, 1296–1305. https://doi.org/10.1039/C5PP00152H
38. Khalid, M., M. A. Oliveira, S. P. Souza, L. F. M. L. Ciscato, F. H. Bartoloni and W. J. Baader (2015) Efficiency of intermolecular chemiluminescence systems lacks significant solvent cavity effect in binary toluene/diphenylmethane mixtures. *J. Photochem. Photobiol. A Chem.* **312**, 81–87. https://doi.org/10.1016/j.jphotochem.2015.06.031
39. Khalid, M., S. P. de Souza, F. H. Bartoloni, F. A. Augusto and W. J. Baader (2016) Chemiexcitation efficiency of intermolecular electron-transfer catalyzed peroxide decomposition shows low sensitivity to solvent-cavity effects. *Photochem. Photobiol.* **92**, 537–545. https://doi.org/10.1111/php.12599
40. Catherallt, C. L. R. and T. F. Palmer (1989) Determination of absolute chemiluminescence quantum yields for reactions of bis-(pentachlorophenyl) oxalate, hydrogen peroxide and fluorescent compounds. *J. Biolumin. Chemilumin.* **3**, 147–154. https://doi.org/10.1002/bio.1170030308
41. Stevani, C. V., S. M. Silva and W. J. Baader (2000) Studies on the mechanism of the excitation step in Peroxyoxalate chemiluminescence. *European J. Org. Chem.*, 4037–4046. https://doi.org/10.1002/1099-0690(200012)2000:24<4037::AID-EJOC4037>3.0.CO;2-A
42. Silva, S. M., K. Wagner, D. Weiss, R. Beckert, C. V. Stevani and W. J. Baader (2002) Studies on the chemiexcitation step in peroxyoxalate chemiluminescence using steroid-substituted activators. *Luminescence* **17**, 362–369. https://doi.org/10.1002/bio.694
43. Souza, S. P., M. Khalid, F. A. Augusto and W. J. Baader (2016) Peroxyoxalate chemiluminescence efficiency in polar medium is moderately enhanced by solvent viscosity. *J. Photochem. Photobiol. A Chem.* **321**, 143–150. https://doi.org/10.1016/j.jphotochem.2016.02.001
44. Ciscato, L. F. M. L., F. H. Bartoloni, E. L. Bastos and W. J. Baader (2009) Direct kinetic observation of the chemiexcitation step in peroxyoxalate chemiluminescence. *J. Org. Chem.* **74**, 8974–8979. https://doi.org/10.1021/jo901402k
45. Catherall, C. L. R., D. T. F. Palmer and R. B. Cundall (1984) Chemiluminescence from reactions of bis(pentachlorophenyl)oxalate, hydrogen peroxide and fluorescent compounds kinetics and mechanism. *J. Chem. Soc. Faraday Trans.* **80**, 823–834. https://doi.org/10.1039/f29848000823
46. Schaap, A. P. and S. D. Gagnon (1982) Chemiluminescence from a phenoxide-substituted 1,2-dioxetane: A model for firefly bioluminescence. *J. Am. Chem. Soc.* **104**, 3504–3506. https://doi.org/10.1021/ja00376a044
47. Schaap, A. P., M. D. Sandison and R. S. Handley (1987) Chemical and enzymatic triggering of 1,2-dioxetanes. 3: Alkaline phosphatase-catalyzed chemiluminescence from an aryl phosphate-substituted dioxetane. *Tetrahedron Lett.* **28**, 1159–1162. https://doi.org/10.1016/S0040-4039(00)95314-0
48. Schaap, A. P., T. Chen, R. S. Handley, R. DeSilva and B. P. Giri (1987) Chemical and enzymatic triggering of 1,2-dioxetanes. 2: Fluoride-induced chemiluminescence from tert-butyldimethylsilyloxy-substituted dioxetanes. *Tetrahedron Lett.* **28**, 1155–1158. https://doi.org/10.1016/S0040-4039(00)95313-9
49. Schaap, A. P., R. S. Handley and B. P. Giri (1987) Chemical and enzymatic triggering of 1,2-dioxetanes. 1: Aryl esterase-catalyzed chemiluminescence from a naphthyl acetate-substituted dioxetane. *Tetrahedron Lett.* **28**, 935–938. https://doi.org/10.1016/S0040-4039(00)95878-7
50. Augusto, F. A., G. A. De Souza, S. P. De Souza, M. Khalid and W. J. Baader (2013) Efficiency of electron transfer initiated chemiluminescence. *Photochem. Photobiol.* **89**, 1299–1317. https://doi.org/10.1111/php.12102
51. Nery, A. L. P., S. Röpke, L. H. Catalani and W. J. Baader (1999) Fluoride-triggered decomposition of m-sililoxyphenyl-substituted dioxetanes by an intramolecular electron transfer (CIEEL) mechanism. *Tetrahedron Lett.* **40**, 2443–2446. https://doi.org/10.1016/S0040-4039(99)00236-1
52. Nery, A. L. P., D. Weiss, L. H. Catalani and W. Baader (2000) Studies on the intramolecular electron transfer catalyzed thermolysis of 1,2-dioxetanes. *Tetrahedron* **56**(30), 5317–5327. https://doi.org/10.1016/S0040-4020(00)00457-9
53. Matsumoto, M. (2004) Advanced chemistry of dioxetane-based chemiluminescent substrates originating from bioluminescence. *J. Photochem. Photobiol. C Photochem. Rev.* **5**, 27–53. https://doi.org/10.1016/j.jphotochemrev.2004.02.001
54. Beck, S. and H. Köster (1990) Applications of dioxetane chemiluminescent probes to molecular biology. *Anal. Chem.* **62**, 2258–2270. https://doi.org/10.1021/ac00220a003
55. Green, O., T. Eilon, N. Hananya, S. Gutkin, C. R. Bauer and D. Shabat (2017) Opening a gateway for chemiluminescence cell imaging: Distinctive methodology for design of bright chemiluminescent dioxetane probes. *ACS Cent. Sci.* **3**, 349–358. https://doi.org/10.1021/acscentsci.7b00058
56. Haris, U., H. N. Kagalwala, Y. L. Kim and A. R. Lippert (2021) Seeking illumination: The path to chemiluminescent 1,2-dioxetanes for quantitative measurements and in vivo imaging. *Acc. Chem. Res.* **54**, 2844–2857. https://doi.org/10.1021/acs.accounts.1c00185
57. Ciscato, L. F. M. L., F. H. Bartoloni, D. Weiss, R. Beckert and W. J. Baader (2010) Experimental evidence of the occurrence of intramolecular electron transfer in catalyzed 1,2-dioxetane decomposition. *J. Org. Chem.* **75**, 6574–6580. https://doi.org/10.1021/jo1013405
58. Bastos, E. L., S. M. Da Silva and W. J. Baader (2013) Solvent cage effects: Basis of a general mechanism for efficient chemiluminescence. *J. Org. Chem.* **78**, 4432–4439. https://doi.org/10.1021/jo400426y
59. Adam, W., M. Matsumoto and A. V. Trofimov (2000) Viscosity dependence of the chemically induced electron-exchange chemiluminescence triggered from a bicyclic dioxetane. *J. Am. Chem. Soc.* **122**, 8631–8634. https://doi.org/10.1021/ja000408w
60. Adam, W. and A. V. Trofimov (2000) The effect of meta versus Para substitution on the efficiency of chemiexcitation in the chemically triggered electron-transfer-initiated decomposition of spiroadamantyl dioxetanes. *J. Org. Chem.* **65**, 6474–6478. https://doi.org/10.1021/jo000495a
61. Alvarez, F. J., N. J. Parekh, B. Matuszewski, R. S. Givens, T. Higuchi and R. L. Schowen (1986) Multiple intermediates generate fluorophore-derived light in the oxalate/peroxide chemiluminescence system. *J. Am. Chem. Soc.* **108**, 6435–6437. https://doi.org/10.1021/ja00280a078
62. Orlovic, M., R. L. Schowen, R. S. Givens, F. Alvarez, B. Matuszewski and N. Parekh (1989) A simplified model for the dynamics of chemiluminescence in the oxalate-hydrogen peroxide system: Toward a reaction mechanism. *J. Org. Chem.* **54**, 3606. https://doi.org/10.1021/jo00276a021
63. Hadd, A. G., A. L. Robinson, K. L. Rowlen and J. W. Birks (1998) Stopped-flow kinetics investigation of the imidazole-catalyzed Peroxyoxalate chemiluminescence reaction. *J. Org. Chem.* **63**, 3023–3031. https://doi.org/10.1021/jo9722109
64. Hadd, A. G., A. Seeber and J. W. Birks (2000) Kinetics of two pathways in peroxyoxalate chemiluminescence. *J. Org. Chem.* **65**, 2675. https://doi.org/10.1021/jo9917487
65. Neuvonen, H. (1997) A two - intermediate model for imidazole – promoted Peroxyoxalate chemiluminescence. *J. Biolumin. Chemilumin.*, **12**, 241–248. https://doi.org/10.1002/(SICI)1099-1271(199709/10)12:5<241::AID-BIO449>3.0.CO;2–3
66. Silva, S. M., F. Casallanovo, K. H. Oyamaguchi, L. F. L. M. Ciscato, C. V. Stevani and W. J. Baader (2002) Kinetic studies on the peroxyoxalate chemiluminescence reaction: Determination of the cyclization rate constant. *Luminescence* **17**, 313–320. https://doi.org/10.1002/bio.693
67. Stevani, C. V, Lima, D. F., Toscano, V. G. and Baader, W. J. (1996) Kinetic studies on the peroxyoxalate chemiluminescent reaction: Imidazole as a nucleophilic catalyst. *J. Chem. Soc. Trans.* **2** 989–995.https://doi.org/10.1039/P29960000989
68. Koike, R., J. Motoyoshiya, Y. Takaguchi and H. Aoyama (2003) The key intermediates that interact with the fluorophores in the peroxyoxalate chemiluminescence reaction of 2,4,6-trichlorophenyl N-aryl-N-tosyloxamates. *Chem. Commun.* **3**, 794–795. https://doi.org/10.1039/b300079f
69. Maruyama, T., S. Narita and J. Motoyoshiya (2013) The Hammett correlation between distyrylbenzene substituents and

chemiluminescence efficiency providing various ρ-values for peroxyoxalate chemiluminescence of several oxalates. *J. Photochem. Photobiol. A Chem.* **252**, 222–231. https://doi.org/10.1016/j.jphotochem.2012.12.006
70. Cabello, M. C. and J. W. Baader (2021) Water effect on peroxyoxalate kinetics and mechanism for oxalic esters with distinct reactivities. *Photochem. Photobiol.* **97**, 1023–1031. https://doi.org/10.1111/php.13445
71. Cabello, M. C., L. V. Bello and W. J. Baader (2020) Use of coumarin derivatives as activators in the peroxyoxalate system in organic and aqueous media. *J. Photochem. Photobiol. A Chem.* **408**, 113076. https://doi.org/10.1016/j.jphotochem.2020.113076
72. Cabello, M. C., G. A. Souza, L. V. Bello and J. W. Baader (2020) Mechanistic studies on the salicylate-catalyzed Peroxyoxalate chemiluminescence in aqueous medium. *Photochem. Photobiol.* **96**, 28–36. https://doi.org/10.1111/php.13180
73. Augusto, F. A., F. H. Bartoloni, A. P. E. Pagano and W. J. Baader (2020) Mechanistic study of the Peroxyoxalate system in completely aqueous carbonate buffer. *Photochem. Photobiol.* **97**, 309–316.
74. Augusto, F. A., F. H. Bartoloni, M. C. Cabello, A. P. F. dos Santos and W. J. Baader (2019) Kinetic studies on 2,6-lutidine catalyzed peroxyoxalate chemiluminescence in organic and aqueous medium: Evidence for general base catalysis. *J. Photochem. Photobiol. A Chem.* **382**, 111967. https://doi.org/10.1016/j.jphotochem.2019.111967
75. Cabello, M. C., O. A. A. El Seoud and W. J. Baader (2018) Effect of ionic liquids on the kinetics and quantum efficiency of peroxyoxalate chemiluminescence in aqueous media. *J. Photochem. Photobiol. A Chem.* **367**, 471–478. https://doi.org/10.1016/j.jphotochem.2018.08.012
76. Souza, G. A., A. P. Lang and W. J. Baader (2017) Mechanistic studies on the Peroxyoxalate chemiluminescence using sodium salicylate as base catalyst. *Photochem. Photobiol.* **93**, 1423–1429. https://doi.org/10.1111/php.12797
77. Souza, G. A., M. M. M. Peixoto, A. P. F. Santos and W. J. Baader (2016) General acid and base catalysis by phosphate in Peroxyoxalate chemiluminescence. *ChemistrySelect* **1**, 2307–2315. https://doi.org/10.1002/slct.201600436
78. Klippenstein, S. J., V. S. Pande and D. G. Truhlar (2014) Chemical kinetics and mechanisms of complex systems: A perspective on recent theoretical advances. *J. Am. Chem. Soc.* **136**, 528–546. https://doi.org/10.1021/ja408723a
79. Blackmond, D. G. (2005) Reaction progress kinetic analysis: A powerful methodology for mechanistic studies of complex catalytic reactions. *Angew. Chemie – Int. Ed.* **44**, 4302–4320. https://doi.org/10.1002/anie.200462544
80. El Seoud, O. A., W. J. Baader and E. L. Bastos (2016) *Encyclopedia of Physical Organic Chemistry, 5 Volume Set*. Wiley, Chichester. https://doi.org/10.1002/9781118468586
81. Orosz, G. (1989) The role of diaryl oxalates in peroxioxalate chemiluminescence. *Tetrahedron* **45**, 3493–3506. https://doi.org/10.1016/S0040-4020(01)81028-0
82. Orosz, G. and E. Dudar (1991) Unexpected decomposition in the reaction of bis(2,4-dinitrophenyl) oxalate with water. *Anal. Chim. Acta* **247**, 141–147. https://doi.org/10.1016/S0003-2670(00)83063-9
83. Orosz, G., R. S. Givens and R. L. Schowen (1992) Chemiluminescence arising from the interaction of rubrene with intermediates derived from hydrogen peroxide and bis(2,4-dinitrophenyl) oxalate (DNPO): Quantum yield and carbondioxide yield. *Anal. Chim. Acta* **266**, 219–223. https://doi.org/10.1016/0003-2670(92)85046-9
84. Neuvonen, H. (1995) Neutral hydrolysis and imidazole-catalysed decomposition of bis(4-nitrophenyl) oxalate. 1,1′-Oxalyldiimidazole as an intermediate. *J. Chem. Soc. Perkin Trans*, 945–949. https://doi.org/10.1039/P29950000945
85. Neuvonen, H. (1994) Kinetics of the decomposition of a chemiluminescent reagent bis(2,4-dinitrophenyI) oxalate in aqueous acetonitrile. *J. Chem. Soc. Perkin Trans*, 89–95. https://doi.org/10.1039/P29940000089
86. Soares, A. R., R. A. Reis, D. U. Melo, A. Boaro and F. H. Bartoloni (2020) Better late than never! Transition state character involved in the neutral solvolysis of an oxalic ester determined by the ionizing power of ethanol/water and methanol/water mixtures. *J. Mol. Liq.* **316**, 113800. https://doi.org/10.1016/j.molliq.2020.113800
87. Kevill, D. N. and M. J. D'Souza (2008) Sixty years of the Grunwald-Winstein equation: Development and recent applications. *J. Chem. Res.*, 61–66. https://doi.org/10.3184/030823408X293189
88. Grunwald, E. and S. Winstein (1948) The correlation of solvolysis rates. *J. Am. Chem. Soc.* **70**, 846–854. https://doi.org/10.1021/ja01182a117
89. Fainberg, A. H. and S. Winstein (1956) Correlation of solvolysis rates. III. T-butyl chloride in a wide range of solvent mixtures. *J. Am. Chem. Soc.* **78**, 2770–2777. https://doi.org/10.1021/ja01593a033
90. Boaro, A. and F. H. Bartoloni (2016) Peroxyoxalate high-energy intermediate is efficiently decomposed by the catalyst imidazole. *Photochem. Photobiol.* **92**, 546–551. https://doi.org/10.1111/php.12608
91. Alves, J., A. Boaro, J. S. Da Silva, T. L. Ferreira, V. B. Keslarek, C. A. Cabral, R. B. Orfão, L. F. M. L. Ciscato and F. H. Bartoloni (2014) Lophine derivatives as activators in peroxyoxalate chemiluminescence. *Photochem. Photobiol. Sci.* **14**, 320–328. https://doi.org/10.1039/c4pp00311j
92. Pedersen, A. D., V. Nielsen and A. Feilberg (2003) Survey of fluorescent substances in consumer products. *Danish Technological Institute*, **2003**, 11–43.
93. Lim, C.-K., Y.-D. Lee, J. Na, J. M. Oh, S. Her, K. Kim, K. Choi, S. Kim and I. C. Kwon (2010) Chemiluminescence-generating nanoreactor formulation for near-infrared imaging of hydrogen peroxide and glucose level in vivo. *Adv. Funct. Mater.* **20**, 2644–2648. https://doi.org/10.1002/adfm.201000780
94. Romanyuk, A. V. and N. S. Melik-Nubarov (2015) Micelles of amphiphilic copolymers as a medium for peroxyoxalate chemiluminescent reaction in water environment. *Polym. Sci. Ser. B* **57**, 360–369. https://doi.org/10.1134/S1560090415040089
95. Feng, J., W. J. Wang, X. Hai, Y. L. Yu and J. H. Wang (2016) Green preparation of nitrogen-doped carbon dots derived from silkworm chrysalis for cell imaging. *J. Mater. Chem. B* **4**, 387–393. https://doi.org/10.1039/c5tb01999k
96. Wang, G., Q. Guo, D. Chen, Z. Liu, X. Zheng, A. Xu, S. Yang and G. Ding (2018) Facile and highly effective synthesis of controllable lattice sulfur-doped graphene quantum dots via hydrothermal treatment of durian. *ACS Appl. Mater. Interfaces* **10**, 5750–5759. https://doi.org/10.1021/acsami.7b16002
97. Chen, D., R. Peng, H. Zhou and H. Liu (2016) Sensitive determination of 4-nitrophenol based on its enhancement of a peroxyoxalate chemiluminescence system containing graphene oxide quantum dots and fluorescein. *Microchim. Acta* **183**, 1699–1704. https://doi.org/10.1007/s00604-016-1799-2
98. Cai, N., D. Q. Yang and F. N. Chen (2019) A novel chemiluminescence system based on bis(2,4,6-Trichlorophyenyl) oxalate and hydrogen peroxide induced by CdTe QDs for determination of phloroglucinol. *Microchem. J.* **144**, 345–350. https://doi.org/10.1016/j.microc.2018.09.024
99. Xie, M., Z. Zhang, W. Guan, W. Zhou and C. Lu (2019) Micelle-mediated chemiluminescence as an indicator for micellar transitions. *Anal Chem* **91**, 2652–2658. https://doi.org/10.1021/acs.analchem.8b03774
100. Motoyoshiya, J. and S. Takigawa (2014) Peroxyoxalate chemiluminescence enhanced by oligophenylenevinylene fluorophores in the presence of various surfactants. *Luminescence* **29**, 772–778. https://doi.org/10.1002/bio.2619
101. Li, Z., Z. Li, D. Li, H. Gao, X. Chen, L. Cao and Y. Hou (2015) Molecularly imprinted polymer-based chemiluminescence imaging assay for the determination of ethopabate residues in chicken muscle. *Anal. Methods* **00**, 1–9. https://doi.org/10.1039/C5AY01874A
102. He, T., G. N. Wang, J. X. Liu, W. L. Zhao, J. J. Huang, M. X. Xu, J. P. Wang and J. Liu (2019) Dummy molecularly imprinted polymer based microplate chemiluminescence sensor for one-step detection of Sudan dyes in egg. *Food Chem.* **288**, 347–353. https://doi.org/10.1016/j.foodchem.2019.03.031
103. Christodouleas, D. C., D. L. Giokas, V. Garyfali, K. Papadopoulos and A. C. Calokerinos (2015) An automatic FIA-CL method for the determination of antioxidant activity of edible oils based on peroxyoxalate chemiluminescence. *Microchem. J.* **118**, 73–79. https://doi.org/10.1016/j.microc.2014.08.003
104. Li, L., D. Lin, F. Yang, Y. Xiao, L. Yang, S. Yu and C. Jiang (2021) Gold nanoparticle-based Peroxyoxalate chemiluminescence

system for highly sensitive and rapid detection of thiram pesticides. *ACS Appl. Nano Mater.* **4**, 3932–3939. https://doi.org/10.1021/acsanm.1c00305
105. Juachon, M. J., J. G. Regala, J. M. Marquez and M. X. Bailon (2019) A proposed image-based detection of methamidophos pesticide using peroxyoxalate chemiluminescence system. *Open Chem.* **17**, 270–278. https://doi.org/10.1515/chem-2019-0034
106. Liu, M., Z. Lin and J. Lin (2010) A review on applications of chemiluminescence detection in food analysis. *Anal. Chim. Acta* **670**, 1–10. https://doi.org/10.1016/j.aca.2010.04.039
107. Li, L., T. Yang, J. Yang and X. Zhang (2022) A robust gold nanocluster-peroxyoxalate chemiluminescence system for highly sensitive detection of cyanide in environmental water. *Sens. Actuators B* **353**, 131038. https://doi.org/10.1016/j.snb.2021.131038
108. Amponsaa-karikari, A., N. Kishikawa, K. Ohyama, K. Nakashima and N. Kuroda (2009) Determination of halofantrine and its main metabolite desbutylhalofantrine in rat plasma by high-performance liquid chromatography with on-line UV irradiation and peroxyoxalate chemiluminescence detection. *Biomed. Chromatogr.* **23**, 101–106. https://doi.org/10.1002/bmc.1094
109. Tsunoda, M. and T. Funatsu (2012) Catecholamine analysis with strong cation exchange column liquid chromatography – Peroxyoxalate chemiluminescence reaction detection. *Anal Bioanal Chem* **402**, 1393–1397. https://doi.org/10.1007/s00216-011-5542-x
110. Tsunoda, M., M. Nagayama, T. Funatsu, S. Hosoda and K. Imai (2006) Catecholamine analysis with microcolumn LC-peroxyoxalate chemiluminescence reaction detection. *Clin Chim Acta* **366**, 168–173. https://doi.org/10.1016/j.cca.2005.09.024
111. Dasari, M., D. Lee, V. R. Erigala and N. Murthy (2009) Chemiluminescent PEG-PCL micelles for imaging hydrogen peroxide. *J. Biomed. Mater. Res. - Part A* **89**, 561–566. https://doi.org/10.1002/jbm.a.32430
112. Lee, I., O. Hwang, D. Yoo, G. Khang and D. Lee (2011) Detection of hydrogen peroxide in vitro and in vivo using peroxalate chemiluminescent micelles. *Bull. Korean Chem. Soc.* **32**, 2187–2192. https://doi.org/10.5012/bkcs.2011.32.7.2187
113. Cho, S., O. Hwang, I. Lee, G. Lee, D. Yoo, G. Khang, P. M. Kang and D. Lee (2012) Chemiluminescent and antioxidant micelles as theranostic agents for hydrogen peroxide associated-infl ammatory diseases. *Adv. Funct. Mater.* **22**, 4038–4043. https://doi.org/10.1002/adfm.201200773
114. Guo, H., H. Aleyasin, B. C. Dickinson, R. E. Haskew-Layton and R. R. Ratan (2014) Recent advances in hydrogen peroxide imaging for biological applications. *Cell Biosci.* **4**, 1–10. https://doi.org/10.1186/2045-3701-4-64
115. Lee, D., V. R. Erigala, M. Dasari, J. Yu, R. M. Dickson and N. Murthy (2008) Detection of hydrogen peroxide with chemiluminescent micelles. *Int. J. Nanomed.* **3**, 471–476. https://doi.org/10.2147/IJN.S3728
116. Chen, R., L. Zhang, J. Gao, W. Wu, Y. Hu and X. Jiang (2011) Chemiluminescent nanomicelles for imaging hydrogen peroxide and self-therapy in photodynamic therapy. *J Biomed Biotechnol* **2011**, 1–9. https://doi.org/10.1155/2011/679492
117. Sadeghi Mohammadi, S., Z. Vaezi, B. Shojaedin-Givi and H. Naderi-Manesh (2019) Chemiluminescent liposomes as a theranostic carrier for detection of tumor cells under oxidative stress. *Anal. Chim. Acta* **1059**, 113–123. https://doi.org/10.1016/j.aca.2019.01.045
118. Naczynski, D. J., M. C. Tan, M. Zevon, B. Wall, J. Kohl, A. Kulesa, S. Chen, C. M. Roth, R. E. Riman and P. V. Moghe (2013) Rare-earth-doped biological composites as in vivo shortwave infrared reporters. *Nat. Commun.* **4**, 2199. https://doi.org/10.1038/ncomms3199
119. Seo, Y. H., A. Singh, H. J. Cho, Y. Kim, J. Heo, C. K. Lim, S. Y. Park, W. D. Jang and S. Kim (2016) Rational design for enhancing inflammation-responsive in vivo chemiluminescence via nanophotonic energy relay to near-infrared AIE-active conjugated polymer. *Biomaterials* **84**, 111–118. https://doi.org/10.1016/j.biomaterials.2016.01.038
120. Mao, D., W. Wu, S. Ji, C. Chen, F. Hu, D. Kong, D. Ding and B. Liu (2017) Chemiluminescence-guided cancer therapy using a chemiexcited photosensitizer. *Chem* **3**, 991–1007. https://doi.org/10.1016/j.chempr.2017.10.002
121. Yang, Y., S. Wang, L. Lu, Q. Zhang, P. Yu, Y. Fan and F. Zhang (2020) NIR-II chemiluminescence molecular sensor for in vivo high-contrast inflammation imaging. *Angew. Chemie Int. Ed.* **59**, 18380–18385. https://doi.org/10.1002/anie.202007649
122. Shuhendler, A. J., K. Pu, L. Cui, J. P. Uetrecht and J. Rao (2014) Real-time imaging of oxidative and nitrosative stress in the liver of live animals for drug-toxicity testing. *Nat. Biotechnol.* **32**, 373–380. https://doi.org/10.1038/nbt.2838
123. Singh, A., Y. Hun Seo, C.-K. Lim, J. Koh, W.-D. Jang, I. Chan Kwon and S. Kim (2015) Biolighted Nanotorch capable of systemic self-delivery and diagnostic imaging. *ACS Nano* **9**, 9906–9911. https://doi.org/10.1021/acsnano.5b03377
124. Biparva, P., S. M. Abedirad and S. Y. Kazemi (2015) Silver nanoparticles enhanced a novel TCPO-H2O2-safranin O chemiluminescence system for determination of 6-mercaptopurine. *Spectrochim. Acta – Part A Mol. Biomol. Spectrosc.* **145**, 454–460. https://doi.org/10.1016/j.saa.2015.03.019
125. Zhen, X., C. Zhang, C. Xie, Q. Miao, K. Leong Lim and K. Pu (2016) Intraparticle energy level alignment of semiconducting polymer nanoparticles to amplify chemiluminescence for ultrasensitive in vivo imaging of reactive oxygen species. *ACS Nano* **10**, 6400–6409. https://doi.org/10.1021/acsnano.6b02908
126. Li, Z., B. Zhu, X. Duan and W. Tang (2019) The imaging of local glucose levels in tumor periphery: Via peroxyoxalate chemiluminescent nanoparticle-glucose oxidase-doped alginate hydrogel. *Anal. Methods* **11**, 2763–2768. https://doi.org/10.1039/c9ay00625g
127. Ding, Y., W. Liu, J. Wu, X. Zheng, J. Ge, H. Ren, W. Zhang, C. S. Lee and P. Wang (2021) Ultrasound-enhanced self-exciting photodynamic therapy based on Hypocrellin B. *Chem. – An Asian J.* **16**, 1221–1224. https://doi.org/10.1002/asia.202100205
128. Zhang, C., J. Jin, K. Liu, X. Ma and X. Zhang (2021) Carbon dots-peroxyoxalate micelle as a highly luminous chemiluminescence system under physiological conditions. *Chinese Chem. Lett.* **32**, 3931–3935. https://doi.org/10.1016/j.cclet.2021.05.050
129. Quimbar, M. E., S. Q. Davis, S. T. Al-Farra, A. Hayes, V. Jovic, M. Masuda and A. R. Lippert (2020) Chemiluminescent measurement of hydrogen peroxide in the exhaled breath condensate of healthy and asthmatic adults. *Anal. Chem.* **92**, 14594–14600. https://doi.org/10.1021/acs.analchem.0c02929

AUTHOR BIOGRAPHIES

Maidileyvis C. Cabello was born in La Havana, Cuba, in 1991. She graduated with honors in Radiochemistry from the Higher Institute of Technologies and Applied Sciences (INTEC), Havana, Cuba. She obtained her Ph.D. in Chemistry at the University of São Paulo in 2020 under the supervision of Prof. W. J. Baader, acting mainly on studies on the mechanism of peroxyoxalate chemiluminescence in aqueous media. Currently, she is a postdoctoral researcher in the group of Prof. R. K. Salinas, where she has gained a general experimental background in culture cells, gene cloning, and purification of membrane proteins.

Fernando H. Bartoloni was born in São Caetano do Sul, Brazil, in 1984. He studied Chemistry at the University of São Paulo (B.Sc. in 2006, Ph.D. in 2011). For his thesis, supervised by Prof. Dr. Wilhelm J. Baader, he studied the chemiluminescence of 1,2-dioxetanones and the mechanism of the peroxyoxalate reaction in aqueous media. He became a professor at the Federal University of ABC (UFABC) in 2012, after a period as a postdoc at this same institution, supervised by Prof. Dr. Erick L. Bastos. He is now an adjunct professor at UFABC, working with fluorescence and chemiluminescence.

Wilhelm J. Baader was born in 1954 in Spalt (Germany), and studied Chemistry at the University of Würzburg, where he got his Ph.D. in 1983 under the supervision of Prof. Waldemar Adam, working on the mechanism of 1,2-dioxetane decomposition. After post-doctoral studies at the Universities of São Paulo (Brazil) and Konstanz (Germany), he became a Professor at the University of São Paulo in 1989, and since then he has been working in the field of mechanistic and applied organic chemiluminescence.